MATERIALS CHEMISTRY
FRONTIERS

REVIEW

View Article Online
View Journal | View Issue



Cite this: *Mater. Chem. Front.*, 2024, **8**, 192

# Transition metal ion-doped cesium lead halide perovskite nanocrystals: doping strategies and luminescence design

Yunqin Zhang,[a] Datao Tu, *[ab] Luping Wang,[a] Chenliang Li,[a] Yuhan Liu[a] and Xueyuan Chen *[ab]

Received 20th June 2023,
Accepted 15th September 2023

DOI: 10.1039/d3qm00691c

rsc.li/frontiers-materials

Cesium lead halide perovskite nanocrystals have received considerable attention due to their extraordinary optoelectronic properties including tunable bandgaps over the entire visible spectral region, high photoluminescence quantum yields, and narrow emission band widths. Transition metal ion doping in cesium lead halide perovskite nanocrystals, emerging as an effective method to manipulate the optical properties, is of vital importance for their fundamental research and applications ranging from light-emitting diodes, solar cells, and microlasers to X-ray detection. In this review, we provide an overview of the most recent advances in the design of transition metal ion-doped lead halide perovskite nanocrystals. We briefly introduce several typical strategies for effective doping of transition metal ions in cesium lead halide perovskite nanocrystals. By virtue of transition metal ion doping, we then highlight the manipulation of the optical properties of cesium lead halide perovskite nanocrystals, which includes improving stability, enhancing luminescence efficiency, and tuning emission band and luminescence lifetime. Finally, the challenges and prospects of this active research field are discussed.



## 1. Introduction

Since Protesescu reported the synthesis and optical properties of cesium lead halide perovskite nanocrystals (NCs) in 2015, the last few years have witnessed a rapid development of cesium lead halide perovskite NCs in the fields of luminescent materials, light-emitting diodes (LEDs), solar cells, photodetectors, scintillators and ferroelectrics.[1–6] Cesium lead halide perovskite NCs are usually represented by $CsPbX_3$ (X = Cl, Br, or I) with a three-dimensional crystal structure or $Cs_4PbX_6$ (X = Cl, Br, or I) with a zero-dimensional crystal structure. Although much progress has been made in cesium lead halide perovskites, some baffling problems like the high toxicity of $Pb^{2+}$ and poor structural stability severely restricted their fundamental research and applications. In this regard, various strategies were proposed, including adjusting their composition, exploring new reaction routes, passivating their surface traps with organic molecules or inorganic salts, and constructing hybrid systems with other materials.[7–10] Currently, cation doping especially transition metal ion doping is frequently proposed to tune their composition and optimize their optical properties for versatile applications.[11–15]

[a] *CAS Key Laboratory of Design and Assembly of Functional Nanostructures, Fujian Key Laboratory of Nanomaterials, and State Key Laboratory of Structural Chemistry, Fujian Institute of Research on the Structure of Matter, Chinese Academy of Sciences, Fuzhou, Fujian 350002, China. E-mail: dttu@fjirsm.ac.cn, xchen@fjirsm.ac.cn*
[b] *Fujian Science & Technology Innovation Laboratory for Optoelectronic Information of China, Fuzhou, Fujian 350108, China*

*Yunqin Zhang earned his B.Sc. degree (2015) in Chemistry from Soochow University. He received his PhD (2021) in Condensed Matter Physics from Fujian Institute of Research on the Structure of Matter (FJIRSM), Chinese Academy of Sciences (CAS). He joined Prof. Xueyuan Chen's group as a postdoctoral associate in 2021. His research focuses on the controlled synthesis and optical properties of inorganic luminescent materials, including lanthanide ions doped nanocrystals, lead halide perovskite nanocrystals and lead-free halide nanocrystals.*

*Datao Tu earned his B.Sc. (2006) from the Wuhan University of Technology. He received his PhD (2011) in Materials Physics and Chemistry from FJIRSM, CAS. He joined Prof. Xueyuan Chen's group as a research assistant professor in 2011 and was promoted to a research professor in 2020. His research interest is focused on the chemical synthesis, optical spectroscopy and bioapplications of inorganic nanocrystals.*

 

Transition metal ions are employed to modulate the photophysical properties of cesium lead halide perovskite NCs by tuning the crystal growth kinetics, changing the crystal structure, or regulating their excited-state dynamics.[16–18] Due to the chemical properties and electronic energy level structure, several kinds of transition metal ions are found to be suitable for doping in cesium lead halide perovskite NCs, including $Mn^{2+}$, $Ni^{2+}$, $Cd^{2+}$, $Zn^{2+}$, $Ag^{+}$, and $Cu^{+}$, to name a few.[19,20] Among these ions, some cations (*e.g.*, $Mn^{2+}$, $Cd^{2+}$) exhibit distinct luminescence, which are utilized as "optically active ions", while other cations (*e.g.*, $Zn^{2+}$, $Ag^{+}$) are usually "non-optically active ions". When optically active ions are doped into cesium lead halide perovskite NCs, a new emission band may appear. Meanwhile, the exciton emission would be decreased or quenched due to the competition between energy transfer and radiative recombination.[21] Generally, since the radii of these transition metal ions are smaller than those of $Pb^{2+}$ ions, the bandgaps of the cesium lead halide perovskite NCs usually get wider upon doping. Correspondingly, the PL peak may blue shift with widening the bandgap.[22] Moreover, transition metal ions may alter the near-band-edge states by eliminating the halide vacancies on the surface. Thus, the PL intensity and stability can be enhanced due to the elimination of these surface trap states.[23–27]

Cesium lead halide perovskite NCs have shown great promise in versatile applications ranging from LEDs, solar cells, and microlasers to X-ray detection.[15,28] Under operating conditions, cesium lead halide perovskite NCs face substantial challenges such as strong light irradiation, applied electric field, unbalanced charge-injection and transport. Doping with transition metal ions is an effective way to improve the efficiency and stability of these NCs to fulfill the requirements of diverse applications.[29] For example, in solar cells, transition metal ion doping can modify the optoelectrical properties including charge carrier recombination rate, diffusion length and contact resistance, as well as the open circuit voltage, resulting in improved device performance in terms of power conversion efficiency and operational stability.[30,31] For LED applications, transition metal ion-doped $CsPbX_3$ NCs can function as efficient light emitters to fabricate high-performance LEDs with higher luminance and external quantum efficiency than their pure counterparts, by eliminating surface defects and promoting the balance of charge carrier mobilities.[32–36] So far, various transition metal ion-doped cesium lead halide perovskite NCs have been explored for multicolor LED applications.[14,26,37] For instance, $CsPb(Cl/Br)_3$:$Ni^{2+}$, $CsPbBr_3$:$Mn^{2+}$, and $CsPbI_3$:$Zn^{2+}$ were employed in blue-emitting LEDs, green-emitting LEDs and red-emitting LEDs, respectively.[35,38,39]

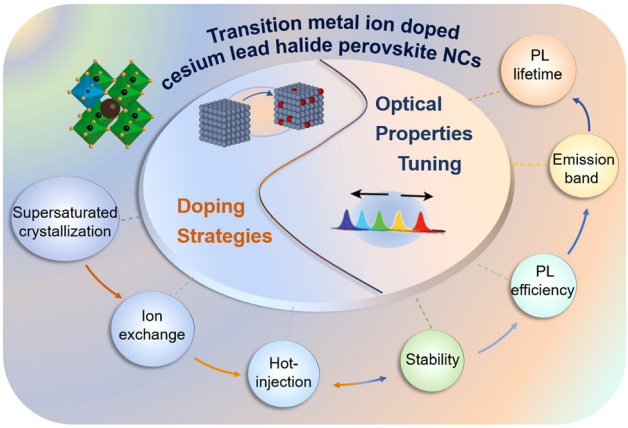


Fig. 1 Overview of transition metal ions doped cesium lead halide perovskite NCs from doping strategies to optical properties manipulation.

Hitherto, several critical and tutorial reviews have summarized the development of controlled syntheses and regulation of the optical properties of cesium lead halide perovskite NCs.[6,40–45]

*Luping Wang earned her B.Sc. degree (2019) in Inorganic Non-Metallic Materials from Shandong University. She is currently a PhD candidate at the University of Chinese Academy of Sciences and studies at FJIRSM, CAS under the supervision of Prof. Xueyuan Chen. Her research focuses on the controlled synthesis and optical properties of inorganic luminescent materials, including lanthanide upconversion nanocrystals and lead-free halide perovskites.*

*Chenliang Li earned his B.Sc. degree (2020) in Applied Chemistry from Shandong University. He is currently a PhD candidate at Shanghaitech University and studies at FJIRSM, CAS under the supervision of Prof. Xueyuan Chen. His research focuses on the controlled synthesis and optical properties of inorganic luminescent materials, including lanthanide upconversion nanocrystals and lead-free halide perovskites.*

*Yuhan Liu earned her B.Sc. degree (2021) in Polymer materials and engineering from Jining University. She is currently a M.S. candidate at Fuzhou University and studies at FJIRSM, CAS under the supervision of Prof. Xueyuan Chen. Her research focuses on the controlled synthesis and optical properties of lead-free halide perovskites.*

*Xueyuan Chen is the editor-in-chief of the Journal of Luminescence. He earned his B.Sc. degree (1993) from the University of Science and Technology of China and his PhD degree (1998) from FJIRSM, CAS. From 2001 to 2005, he was a postdoctoral research associate at the Chemistry Division of Argonne National Laboratory, U.S. Department of Energy, where he studied the photophysics and photochemistry of heavy elements. In 2005, he joined the faculty of FJIRSM, where he is currently a professor and group leader in materials chemistry and physics. His research focuses on the electronic structures, optical properties, and applications of inorganic luminescent materials, such as lanthanide-doped nanoprobes, LED phosphors, and low-dimensional metal-halide perovskites.*

However, there have been few reviews focusing on transition metal ion-doped cesium lead halide perovskite NCs. It is urgent to renew the knowledge about the design of transition metal ion-doped cesium lead halide perovskite NCs because more new understanding or progress has been gained very recently. Rather than being exhaustive, this review aims to highlight the doping strategies and manipulation of the optical properties of transition metal ion-doped cesium lead halide perovskite NCs. This review is organized as follows (Fig. 1). First, the doping strategies of transition metal ions in cesium lead halide perovskite NCs are surveyed, with an emphasis on the hot-injection method, ion exchange method and supersaturated crystallization method. Then, the optical properties manipulation of cesium lead halide perovskite NCs through doping with transition metal ions is systematically discussed, including improving the stability, enhancing the luminescence efficiency, tuning the emission band and tuning the luminescence lifetime. Finally, emerging trends and further efforts are proposed.

## 2. Doping strategies

Because of the fast nucleation and growth process of cesium lead halide perovskite NCs, the controlled doping of transition metal ions remains a challenge.[46] Theoretically, transition metal ions can be doped at the A-site ($Cs^+$) or the B-site ($Pb^{2+}$) of $CsPbX_3$ NCs by *in situ* synthesis or post-synthesis approaches.[47] Nowadays, the hot-injection method and post-synthetic cation exchange method are two commonly used methods for the preparation of high-quality transition metal ion-doped cesium lead halide NCs (Table 1).

Very recently, other doping strategies including supersaturated crystallization, ligand-assisted ultrasonication, mechanosynthesis, host phase transition method, and modular microfluidics method are proposed.[48–51] Supersaturated crystallization and ligand-assisted ultrasonication are both carried out in solution at ambient atmosphere. Supersaturated crystallization utilizes the solubility difference of perovskite solutions in polar solvents and non-polar solvents.[52] The ligand-assisted ultrasonication method is a versatile, polar-solvent-free, single-step approach based on the direct ultrasonication of the corresponding precursors in the presence of organic ligands.[53] Through mechanosynthesis, powder products can be obtained without using polar solvents, where $CsPbX_3$ NCs are prepared using a planetary ball mill with the addition of ligands.[54] The modular microfluidics method involves the injection of two or more component liquids (*e.g.*, droplets) into capillary channels of the automated modular microfluidic platform, where the chemical composition and morphology of the samples can be tailored.[51,55]

In this section, we will briefly illustrate the doping strategies of the hot-injection method, cation exchange method and supersaturated crystallization method, which were widely employed.

### 2.1. Hot-injection method

**Cs-oleates approach.** The hot-injection method was first reported by Protesescu *et al.* for the synthesis of $CsPbX_3$ NCs.[1] Using this method, $Mn^{2+}$ was successfully doped in $CsPbCl_3$ NCs by the Son group and the Klimov group, respectively (Fig. 2a).[56,57] In their reports, metal cation precursors with a [Mn]/[Pb] ratio of 0.25 to 1.5 were dissolved in octadecene and ligands (*e.g.*, oleic acid and oleylamine). Meanwhile, $Cs_2CO_3$ was dissolved in oleic acid upon heating to obtain Cs-oleate solutions, which were rapidly injected into the metal cation precursor solutions with stirring and heating at 120–185 °C, followed by fast cooling. As a result, $CsPbCl_3$:$Mn^{2+}$ NCs with a size of ~11 nm were obtained. Currently, this approach is the most widely reported approach for transition metal ion doping, wherein heating favors crystallization and ligands provide effective protection for cesium lead halide perovskite NCs. Likewise, $CsPb(Cl/Br)_3$:$Mn^{2+}$, $CsPbBr_3$:$Mn^{2+}$ and $CsPbI_3$:$Mn^{2+}$ NCs can be prepared with the precursors of $MnCl_2$/$MnBr_2$, $MnBr_2$, and $MnI_2$, respectively.[58] Besides conventional cesium lead chlorides of $CsPbCl_3$ with 3D structure, $Cs_4PbCl_6$ NCs with 0D structure can also be readily doped with $Mn^{2+}$ *via* the Cs-oleate approach by decreasing the amount of injected Cs-oleates ([Pb]/[Cs] $<0.5$) to avoid $CsPbX_3$ impurities.[59]

Table 1 Typical examples for the doping of transition metal ions in cesium lead halide perovskite NCs

| Host | Dopant | Synthesis strategy | Reaction temperature (°C) | Feed ratio ([dopant]/[Pb]) | Actual doping content | Size (nm) | Ref. |
|---|---|---|---|---|---|---|---|
| $CsPbCl_3$ | $Mn^{2+}$ | hot-injection | 200 | 1 | 0.6% | 7.3–8.6 | 111 |
| $CsPb(Cl_{0.6}Br_{0.4})_3$ | $Mn^{2+}$ | hot-injection | 250 | 5 | 25% | ~19 | 13 |
| $CsPbCl_3$ | $Mn^{2+}$ | cation exchange | 25 | 0.1 | 5.7% | 7.2 | 104 |
| $CsPbCl_3$ | $Mn^{2+}$ | cation exchange | 25 | 100 | 5.7% | 16.7 | 47 |
| $CsPbI_3$ | $Ni^{2+}$ | ion exchange | 25 | 0.5 | 1.38% | 15 | 76 |
| $CsPbBr_3$ | $Ni^{2+}$ | hot-injection | 180 | 2.5 | — | 14-15 | 17 |
| $CsPbCl_3$ | $Ni^{2+}$ | hot-injection | 210 | 2 | 11.9% | 8.3 | 78 |
| $CsPbBr_3$ | $Cd^{2+}$ | hot-injection | 220 | 4 | 0.92% | 84 × 16 | 134 |
| $CsPbBr_3$ | $Cd^{2+}$ | hot-injection | 170 | 2 | 7% | 10.21 | 81 |
| $CsPbCl_3$ | $Zn^{2+}$ | hot-injection | 210 | 1.5 | 8.6% | 8.4–9.73 | 79 |
| $CsPbBr_3$ | $Zn^{2+}$ | hot-injection | 90 | 2 | — | 13.1 | 73 |
| $CsPbCl_3$ | $Cu^{2+}$ | hot-injection | 185 | 1.17 | 7% | 7.0 | 75 |
| $CsPb(Cl/Br)_3$ | $Cu^{+}$ | anion exchange | 25 | ~7.3 | — | 10 | 21 |
| $CsPb(Cl/Br)_3$ | $Cu^{2+}$ | anion exchange | 25 | ~3.65 | — | 10 | 21 |
| $CsPb(Br/I)_3$ | $Ag^{+}$ | hot-injection | 25 | 0.04 | 3.5% | 8.1–8.4 | 24 |
| $CsPbBrI_2$ | $Fe^{2+}$ | hot-injection | 160 | 0.5 | 2.4% | 15.2–18.5 | 25 |
| $Cs_4PbCl_6$ | $Mn^{2+}$ | hot-injection | 180 | 0.25 | 23.6^ | 20 | 92 |

 

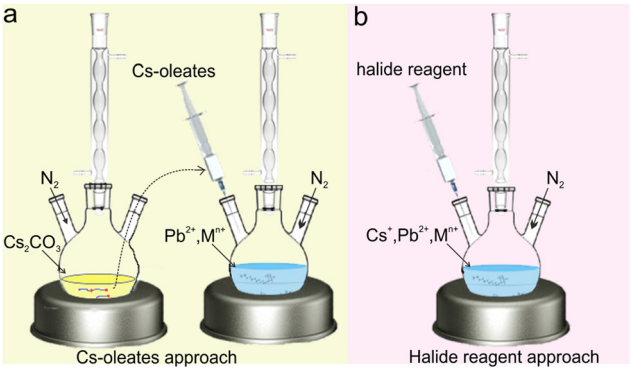


Fig. 2 (a) Schematic illustration for the synthesis of transition metal ion-doped cesium lead halide perovskite NCs *via* hot injection method based on (a) Cs-oleates approach and (b) halide reagent approach.

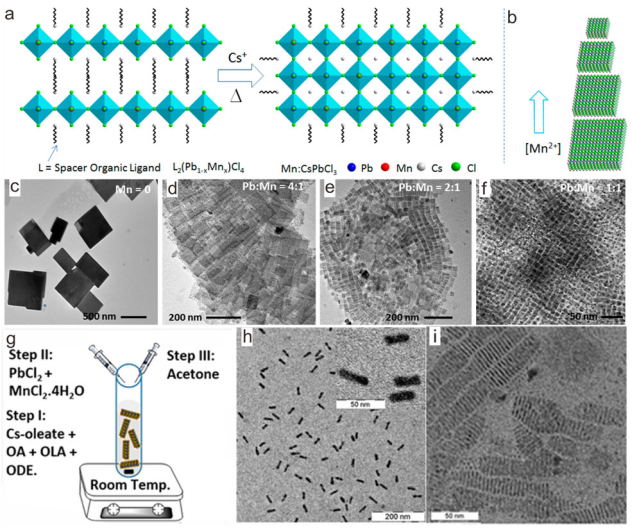


Fig. 3 (a) Schematic illustration of the formation of $CsPbCl_3$:$Mn^{2+}$ nanoplates from layered perovskites $L_2(Pb_{1-x}Mn_x)Cl_4$, wherein L is *n*-butylammonium and oleylammonium ions. (b) Schematic illustration shows $Mn^{2+}$ concentration in the reaction mixture with different sizes of $CsPbCl_3$:$Mn^{2+}$ NCs. Transmission electron microscopy (TEM) images of (c) undoped and (d)–(f) $Mn^{2+}$-doped $CsPbCl_3$ nanoplates based on different [Pb]:[Mn] precursor ratios. (g) Schematic shows the synthesis of $CsPbCl_3$:$Mn^{2+}$ nanoplates. OA, OLA, and ODE refer to oleic acid, oleylamine, and 1-octadecene, respectively. (h) TEM image of $CsPbCl_3$:$Mn^{2+}$ nanoplates lying flat on the TEM grid. Inset shows a magnified view. (i) TEM image of self-assembled $CsPbCl_3$:$Mn^{2+}$ nanoplates lying perpendicular to the TEM grid. (a)–(f) Reproduced with permission from ref. 68. Copyright 2019, American Chemical Society; (g)–(i) reproduced with permission from ref. 69. Copyright 2020, American Chemical Society.

To increase the doping concentration of $Mn^{2+}$ in cesium lead halide perovskite NCs, the feed ratio of [Mn]/[Pb] precursors and the reaction temperature were investigated. Specifically, when the feed ratio of [Mn]/[Pb] precursors was increased from 1.25 to 10 at a reaction temperature of 170 °C, the $Mn^{2+}$ doping concentration can be increased from 2% to 27%.[60,61] Because $Mn^{2+}$ doping is a thermodynamically controlled process, a high reaction temperature may facilitate the replacement of $Pb^{2+}$ with $Mn^{2+}$ in cesium lead halide perovskite NCs. When the reaction temperature was elevated from 170 °C to 210 °C with the feed [Mn]/[Pb] precursor ratio of 10, the doping concentration of $Mn^{2+}$ can be further increased from 27% to 46%.[62] However, such reaction protocols with a high feed ratio of [Mn]/[Pb] precursors may form byproducts like CsCl or $PbCl_2$, which should be avoided.[63,64]

In addition, the concentration of $Cl^-$ in precursors is also essential for the doping content of transition metal ions in $CsPbCl_3$ NCs.[65] For the preparation of $Mn^{2+}$-doped $CsPbCl_3$ NCs, $MnCl_2$ was found to be more efficient relative to several other manganese salts such as $Mn(Ac)_2$ (Ac: acetate), $Mn(acac)_2$ (acac: acetylacetone), or $Mn(oleate)_2$. The main reason is the similar bond dissociation energy of Mn–Cl (338 kJ $mol^{-1}$) and Pb–Cl (301 kJ $mol^{-1}$).[57] Despite this, the doping efficiency of $Mn^{2+}$ is relatively low, where the precursor with a [Mn]/[Pb] ratio of 1.5 may only result in ~0.2% $Mn^{2+}$ in the obtained $CsPbCl_3$:$Mn^{2+}$ NCs.[56] To promote the effective doping of $Mn^{2+}$ in cesium lead halide NCs, a chloride-rich high-temperature reaction was designed, where several chloride chemicals like alkylamine hydrochloride, trimethylchlorosilane, or $CuCl_2$ was used along with $Mn^{2+}$ salts such as $Mn(Ac)_2$ or $MnCl_2$.[13,63,66,67] By employing alkylamine hydrochloride, the doping content of $Mn^{2+}$ in the obtained $CsPbCl_3$:$Mn^{2+}$ NCs can be as high as 1.3% with a low [Mn]/[Pb] precursor ratio of 0.05. In another report, trimethylchlorosilane was used to promote the formation of both octahedral structural units $[PbCl_6]^{4-}$ and $[MnCl_6]^{4-}$ in the solution before $Cs^+$ injection. Correspondingly, the $Mn^{2+}$ doping content was determined to be 10.3% in the obtained $CsPbCl_3$:$Mn^{2+}$ NCs with a [Mn]/[Pb] precursor ratio of 1.0.

The as-prepared transition metal ion-doped $CsPbX_3$ samples are usually cube-shaped NCs. To tune their morphology, a thermal conversion strategy was explored to synthesize $CsPbCl_3$ nanoplates.[68–71] As a typical example, Das Adhikari *et al.* demonstrated that $CsPbCl_3$:$Mn^{2+}$ nanoplates with tunable size can be obtained through thermal conversion from $Mn^{2+}$-contained layered perovskites.[50] In their report, butylammonium chloride, $PbCl_2$, $MnCl_2$ and ligands were dissolved at 160 °C in octadecene under heating and then cooled down to 100 °C to form $L_2Mn_xPb_{1-x}Cl_4$ (L = *n*-butylammonium and oleylammonium ions) layered perovskites. Then, a hot solution of Cs-oleates was injected. Upon heating at 230 °C, $L_2Mn_xPb_{1-x}Cl_4$ was converted to $CsPbCl_3$:$Mn^{2+}$ nanoplates (Fig. 3a). Through adjusting the feed $[Mn^{2+}]/[Pb^{2+}]$ precursor ratio from 0 to 1, the size of the final $CsPbCl_3$:$Mn^{2+}$ nanoplate can be tuned from 580 nm to 20 nm, while the thickness of the platelets remained essentially unchanged (~5 nm) (Fig. 3b–f).

To circumvent the cumbersome procedures for preparing the layered perovskite of $L_2Mn_xPb_{1-x}Cl_4$, a convenient strategy was proposed to directly synthesize $Mn^{2+}$-doped $CsPbCl_3$ nanoplates by utilizing $Cl^-$-rich precursors to confine the nanocrystal growth at the lattice face ⟨001⟩.[51] To dissolve the metal chloride precursors in solutions for high $Cl^-$ content, polar solvents like *N*,*N*-dimethylformamide (DMF) or dimethyl sulfoxide (DMSO) were employed, wherein HCl, $PbCl_2$ and $MnCl_2$ were dissolved to prepare $Cl^-$-rich precursors solution. Such a solution was then injected into a toluene solution containing

Cs-oleates, followed by adding acetone (Fig. 3g). As a result, $CsPbCl_3$:$Mn^{2+}$ nanoplates with a thickness of 2.3 nm were obtained, corresponding to four monolayers of $CsPbCl_3$ (Fig. 3h and i). Inspired by this work, $CsPbCl_3$:$Mn^{2+}$ with hexapod structure was prepared based on oleylamine hydrochloride.[52,53]

Similar to $Mn^{2+}$ doping, the hot-injection method was also applied for the doping of other transition metal cations (*e.g.*, $Ni^{2+}$, $Zn^{2+}$, $Cd^{2+}$, $Cu^{2+}$, $Cu^{+}$, $Ag^{+}$, $Ti^{3+}$, and $Fe^{3+}$) in cesium lead halide perovskite NCs.[14,24,56,72–81] Specifically, copper ion exhibits oxidation numbers of +1 and +2. Generally, $Cu^{2+}$ can be readily doped in $CsPbX_3$ (X = Cl, Br, I or mixture) NCs.[63,82,83] By employing reductive reagents such as trioctylphosphate in the solution, $Cu^{+}$ can be doped into $CsPbCl_3$ NCs.[75]

Interestingly, the selection of transition metal precursors may result in different doping sites of transition metal ions in $CsPbX_3$ NCs. In a recent report, two kinds of $Zn^{2+}$ doping sites were achieved in $CsPbI_3$:$Zn^{2+}$ NCs. Specifically, it was discovered that $Zn^{2+}$ dopants may substitute the $Pb^{2+}$ site in $CsPbI_3$ using $ZnI_2$ precursors, which improved the local ordering of the lattice and reduced the octahedral distortions as confirmed by X-ray absorbance fine structure spectra and X-ray absorption near-edge structure spectra.[84] Nevertheless, using non-halide zinc salts (*e.g.*, zinc acetylacetonate) may lead to doping of $Zn^{2+}$ in the interstitial sites, thus causing lattice expansion as confirmed by the powder X-ray diffraction (XRD) patterns and pair distribution function analyses.[36]

**Halide reagent approach.** In the above-mentioned Cs-oleates approach, $Cs_2CO_3$ and metal cations precursors have to be separately dissolved upon heating. Alternatively, a convenient approach named the "halide reagent approach" was proposed by avoiding the separate preparation of hot Cs-oleate and metal cation solutions. Typically, $Cs_2CO_3$, $Pb(Ac)_2$ and transition metal acetates are dissolved in hot octadecene with ligands of oleic acid and oleylamine to form a cation precursor solution, into which halide reagents such as hydrogen chloride, benzoyl chloride, phenylphosphoryl chloride, or trimethylchlorosilane are injected to synthesize transition metal ion-doped cesium lead halide perovskite NCs (Fig. 2b). In this approach, it is facile to manipulate the chemical composition of [X]/[Pb] in the obtained $CsPbX_3$ NCs, because of the separation of B-site ions (*e.g.*, $Pb^{2+}$, $Mn^{2+}$) and halide ions (*e.g.*, $Cl^{-}$, $Br^{-}$, $I^{-}$) in the precursors.

Since the bromide reagents and iodide reagents (*e.g.*, benzoyl bromide, benzoyl iodide) are usually more volatile, corrosive and highly reactive than chloride reagents (*e.g.*, benzoyl chloride), such an approach using halide reagents was mainly applied for the synthesis of transition metal-doped $CsPbCl_3$ NCs. Benefiting from the benzoyl group or phenylphosphoryl of a halide reagent attached to the surface of NCs, the as-prepared transition metal-doped $CsPbCl_3$ NCs often exhibited high photoluminescence quantum yield (PLQY) (>60%) *via* this approach.[85,86] By contrast, the as-synthesized transition

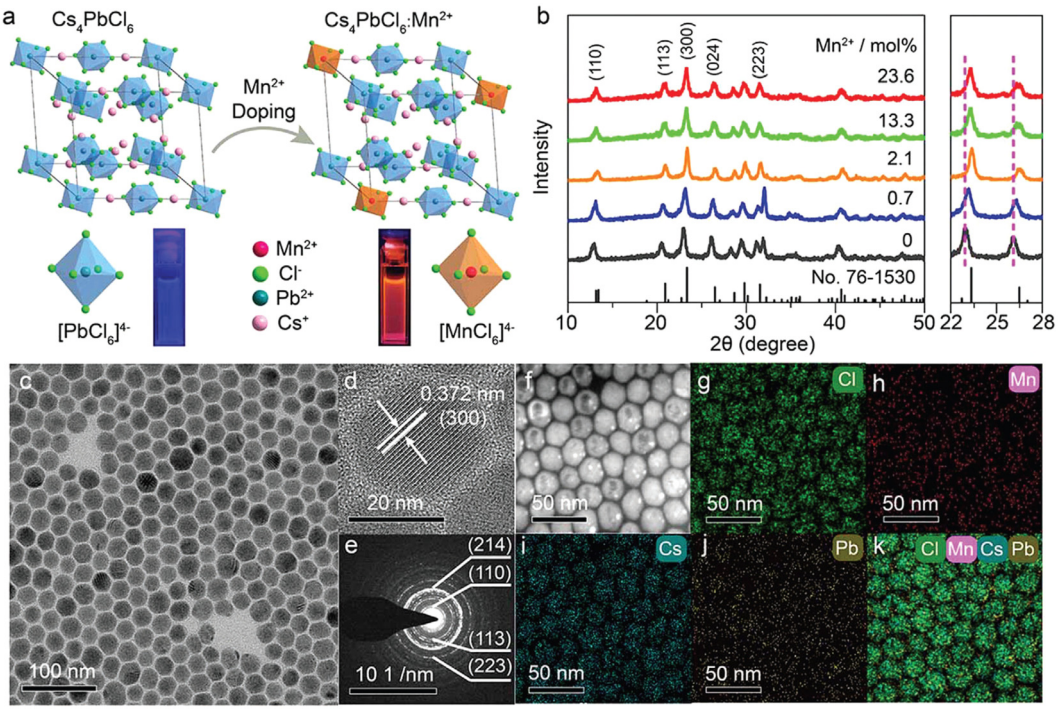


Fig. 4 (a) Crystal structure of rhombohedral $Cs_4PbCl_6$ and the crystallographic site for $Mn^{2+}$ dopants. PL photographs of $Cs_4PbCl_6$ NCs dispersed in cyclohexane under 304 nm ultraviolet lamp irradiation are presented. (b) XRD patterns of $Cs_4PbCl_6$:$Mn^{2+}$ NCs with different $Mn^{2+}$ doping concentrations. Bottom lines represent the standard XRD pattern of rhombohedral $Cs_4PbCl_6$ (JCPDS No. 76-1530). The enlarged $2\theta$ range (22°–28°) of XRD patterns shows a monotonic shift of the diffraction peaks with increasing the $Mn^{2+}$ concentration. (c) TEM image, (d) high-resolution TEM image, (e) selected area electron diffraction pattern, (f) scanning transmission electron microscopy (STEM) image, and (g)–(k) corresponding elemental mappings (Cs, Pb, Mn, and Cl) of $Cs_4PbCl_6$:$Mn^{2+}$ NCs. Reproduced with permission from ref. 92. Copyright 2019, Wiley-VCH Verlag GmbH I Co. KGaA, Weinheim.

 

metal-doped $CsPbCl_3$ NCs through Cs-oleates approach often suffer from relatively low PLQY (~5%).[87,88] Based on the halide reagent approach, $CsPbCl_3$:$Cd^{2+}$ and $CsPbCl_3$:$Mn^{2+}$ NCs with highly efficient emissions were obtained.[89–91]

By virtue of the flexible regulation of the precursor ratio of halide ions and metal ions, we have synthesized $Mn^{2+}$-doped rhombohedral phase $Cs_4PbCl_6$ NCs (Fig. 4).[92] Typically, benzoyl chloride was injected into a hot solution containing $CsCO_3$, $Pb(Ac)_2$ and $Mn(Ac)_2$ with a [benzoyl chloride]/([Pb] + [Mn]) ratio of 6. Benzoyl chloride may release chloride ions very fast at high temperatures. It was discovered that a high [Cl]/[Pb] ratio may be the key to obtaining pure $Cs_4PbCl_6$:$Mn^{2+}$ NCs without the impurities of $CsPbCl_3$. The actual doping concentration of $Mn^{2+}$ in the as-synthesized NCs was tuned from 0.7 mol% to 23.6 mol% by increasing the precursor ratio of [Pb]/[Mn] in the solution. The successful doping of $Mn^{2+}$ into the $Cs_4PbCl_6$ lattice can be confirmed by the PL spectra and XRD patterns (Fig. 4a and b). As shown in the TEM images, the as-prepared $Cs_4PbCl_6$:$Mn^{2+}$ NCs exhibited a hexagonal shape (Fig. 4c–e), which is markedly different from the well-established $CsPbCl_3$:$Mn^{2+}$ NCs. Elemental mapping images indicated that $Mn^{2+}$ ions were distributed uniformly in the obtained NCs (Fig. 4f–k), further confirming the successful doping of $Mn^{2+}$ in the host lattice.

### 2.2. Ion exchange method

In the above-mentioned hot-injection method, doping with transition metal ions is carried out with *in situ* synthesis of the halide perovskite host. As an alternative, doping with transition metal ions can be achieved by a post-synthesis strategy such as ion exchange. The ion (cation or anion) exchange method allows access to a variety of composition and shapes which are not easily attainable through the direct synthesis method.[93–97] For transition metal ion-doped cesium lead halide perovskite NCs, ion exchange generally proceeds in non-polar solutions containing transition metal ion salts (*e.g.*, $MnBr_2$, $ZnBr_2$) and cesium lead halide perovskite NCs. It was demonstrated that halide ion exchange was very efficient and fast in the synthesis of cesium lead halide perovskite NCs.[98] However, cation exchange in early reports usually led to the decomposition of the host NCs when exchanging $Cs^+$ or $Pb^{2+}$ with other guest cations ($Rb^+$, $Ag^+$, $Cu^+$, $Ba^{2+}$, $Sn^{2+}$, $Ge^{2+}$, or $Bi^{3+}$) in $CsPbX_3$ NCs, because the perovskite crystal structure was stabilized primarily by the rigid $[PbX_6]^{4-}$ cationic sublattice. As such, the unbalanced rates of extraction of $Pb^{2+}$ and incorporation of the guest cations resulted in the collapse of the $CsPbX_3$ NCs.[99]

To enable the cation exchange of transition metal ions in $CsPbX_3$ NCs, van der Stam *et al.* proposed a kinetically controlled method, wherein $Pb^{2+}$ ions were partially replaced by divalent cations (*e.g.*, $Sn^{2+}$, $Cd^{2+}$, and $Zn^{2+}$) in $CsPbBr_3$ NCs with a doping content of less than 16% (Fig. 5a).[99] In their work, an oleylamine solution containing metal halides of $MX_2$ (*e.g.*, $ZnBr_2$) was mixed with a $CsPbBr_3$ NC solution with [$M^{2+}$]/[NC] ratio varied between ~8000 and ~300 000. Oleylamine in the solution would aid the formation of halide vacancies on the surface of $CsPbX_3$ NCs. Such halide vacancies can be occupied by $MX_2$, followed by the breaking of the bonds between the

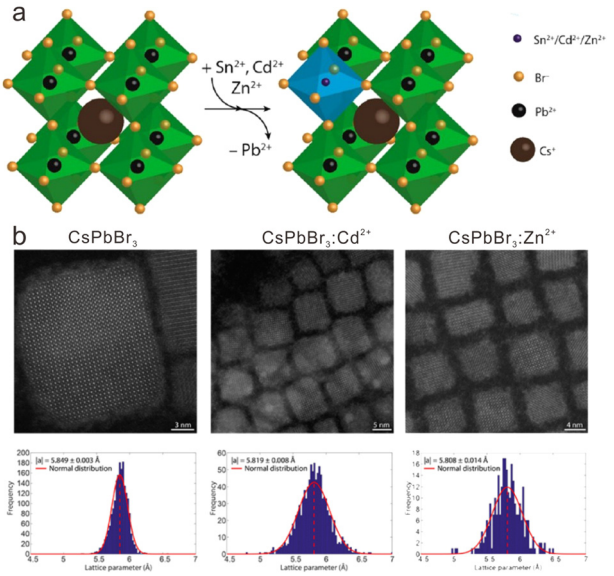


Fig. 5 (a) Schematic illustration of partial cation exchange of host $Pb^{2+}$ with guest $M^{2+}$ ions (M = Mn, Zn and Cd) in $CsPbBr_3$ NCs. (b) Quantitative high-angle annular dark-field STEM images of $CsPbBr_3$, $CsPbBr_3$:$Cd^{2+}$ and $CsPbBr_3$:$Zn^{2+}$. Reproduced with permission from ref. 99. Copyright 2017, American Chemical Society.

surface $PbBr_2$ and the $CsPbBr_3$ NC. Thus, the $Pb^{2+}$ cations on the surface can be exchanged by the $M^{2+}$ guest cations. The obtained $M^{2+}$-doped $CsPbBr_3$ NCs essentially maintained the size and shape as those of the pristine $CsPbBr_3$ NCs (Fig. 5b). By adopting other transition metal halide salts, this method was successfully applied to the doping of $Mn^{2+}$, $Zn^{2+}$ and $Ni^{2+}$ in $CsPb(Br/Cl)_3$ or $CsPbI_3$ NCs.[100–102] However, such a cation exchange reaction usually takes a long time (>16 h) because the surface exchange rate and diffusion fluxes for both the outgoing $Pb^{2+}$ and the incoming $M^{2+}$ cations are slow.

It was demonstrated that surface ligands played an important role in the cation exchange reaction.[103] As such, several ligands were explored to accelerate the exchange rate of $Pb^{2+}$ by transition metal dopants through substantial reduction of the activation energy for the formation of B-site vacancies.[104,105] Utilizing surface ligand exchange with the formation of Lewis acid/base pair, the halide ions attached with $Pb^{2+}$ can be replaced with ligand anions like carbonate. Then, $Pb^{2+}$ can be removed for exchange with transition metal dopants. As a typical example, Yang *et al.* proposed a surface-ligand-exchange-inspired dynamic ion exchange method to accelerate the ion exchange of $Pb^{2+}$ with $Zn^{2+}$ in $CsPbBr_3$ NCs.[106] Generally, the surface of $CsPbBr_3$ NCs is Cs-Br terminated or Br-R-$NH_2^+$ terminated (R is the bulky organic component). Thus, zinc ethylhexanoate ($Zn(Oct)_2$) was employed to promote the departure of surface R-$NH_2^+$ ligands and halide ions, followed by the formation of the surface ion pair Pb-Oct. Such Pb-Oct ion pair was then exchanged by the dopant pair of Zn-Oct on the surface of $CsPbBr_3$ NCs. Such an ion exchange process can be accomplished within serval hours by the ongoing cation diffusion procedure.

Besides the surface ligands, anions were also revealed to promote cation exchange. Compared with cation exchange in

cesium lead halide perovskite NCs, anion exchange is much faster. For example, the anion exchange of $Br^-$ with $Cl^-$ in $CsPbBr_3$ NCs can be readily achieved due to the breaking of the Pb–Br bond and the formation of a Pb–Cl bond. Hence, utilizing the anion exchanged to open up the rigid $[PbX_6]^{4-}$ may favor the cation exchange. To exemplify this, Huang *et al.* dissolved $MnCl_2$ in DMF, which was dropped into a toluene solution containing $CsPbBr_3$ NCs for the synthesis of $Mn^{2+}$-doped $CsPb(Cl/Br)_3$ NCs.[62] They attributed the success of halide-exchange-driven cation exchange to two prerequisites: (i) diffusion of $MnCl_2$ into the $CsPbBr_3$ NC lattice, and (ii) simultaneous existence of halide exchange and cation exchange between $MnCl_2$ and $CsPbBr_3$ NCs. Such a cation exchange process is rapid that can be finished within half an hour.

Initially, the method of halide-exchange-driven cation exchange was mainly applied to $CsPbBr_3$ NCs through direct mixing with dopant salts and ligands. Nevertheless, it was discovered that such a cation exchange may not be achieved in $CsPbCl_3$ NCs by directly mixing with $MnCl_2$ or $MnBr_2$.[107] Fortunately, under light irradiation, cation exchange was realized in a dichloromethane ($CH_2Cl_2$) solution containing $CsPbCl_3$ NCs and transition metal ion salts. The exchange rates can be controlled by excitation light intensity and lasting time. Such a kind of cation exchange is also called "photo-induced doping", which benefits from the process called "self-anion exchange" occurring under light irradiation on the surface of $CsPbCl_3$ NCs in $CH_2Cl_2$. Thus, it provides a convenient and universal approach for doping the surface of $CsPbCl_3$ NCs with transition metal ions. For example, surface doping of several transition metal ions such as $Cu^{2+}$, $Zn^{2+}$, or $Cd^{2+}$ in $CsPbCl_3$ NCs was realized, based on the slow diffusion rate of these transition metal ions in the $CsPbCl_3$ lattice.[21,108,109]

### 2.3. Supersaturated crystallization method

Supersaturated crystallization was also called "ligand-assisted reprecipitation".[110] In principle, it was induced by a change in solubility by mixing $Cs^+$, $Pb^{2+}$ and transition metal precursors in a "good solvent" (high solubility) into a "poor solvent" (low solubility) with ligands at room temperature. The "good solvents" are generally polar solvents such as DMF, DMSO or acetonitrile, while "bad solvents" are weak-polar or non-polar solvents such as toluene, chlorobenzene, *etc.*

For the preparation of $Mn^{2+}$-doped $CsPb(Br/Cl)_3$ NCs, a solution containing high concentrations of CsBr, $PbBr_2$, $MnCl_2$ and ligands in DMF was dropped into toluene with ligands such as oleic acid. Thereafter, $CsPb(Cl/Br)_3$:$Mn^{2+}$ NCs were formed in the mixture solution (Fig. 6a).[52] With increasing the ratio of $[MnCl_2]/[PbBr_2]$ from 0 to 7.5, the $Mn^{2+}$ concentration in the as-prepared $CsPb(Cl/Br)_3$:$Mn^{2+}$ NCs can be elevated to 37.7%. However, the length of the as-prepared $CsPb(Cl/Br)_3$:$Mn^{2+}$ NCs remained at ~11 nm under different feeding ratios of $[MnCl_2]/[PbBr_2]$ (Fig. 6b–e). High-resolution TEM image of the as-prepared $CsPb(Cl/Br)_3$:$Mn^{2+}$ NCs indicated an interplanar distance of 0.56 nm, corresponding to the (100) plane of $CsPb(Cl/Br)_3$ (Fig. 6e). Theoretically, this method does not require heating when the temperature is higher than the melting point of the solvents (the melting points of DMSO and DMF are 19 °C and −61 °C, respectively). Thus, the preparation process is time-saving without cumbersome heating and cooling processes.

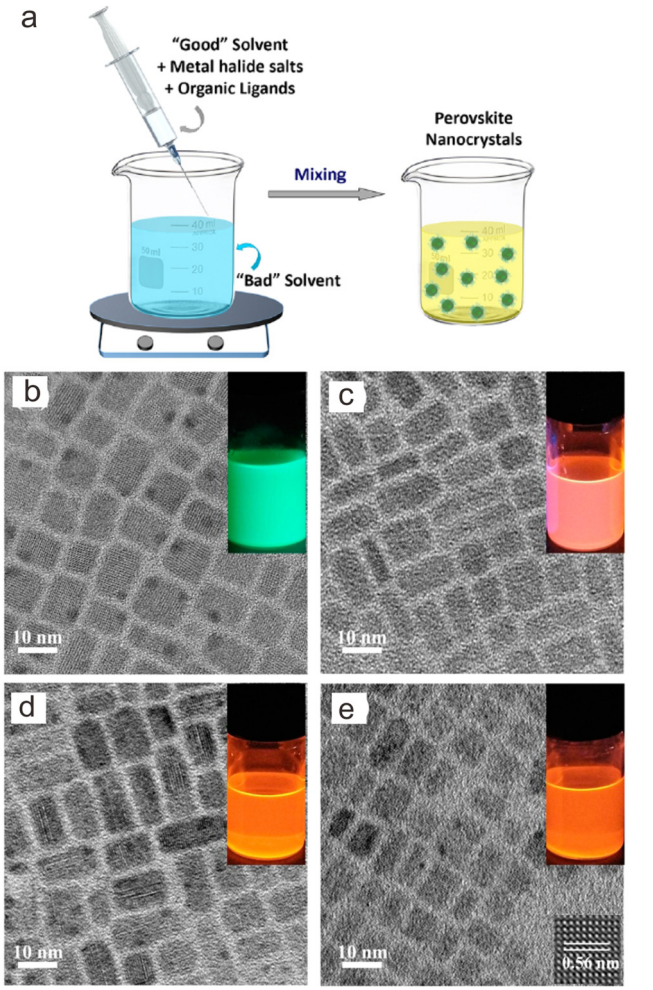


Fig. 6 (a) Schematic illustration of supersaturated crystallization method. TEM images of (b) $CsPbBr_3$ NCs and $CsPb(Cl/Br)_3$:$Mn^{2+}$ NCs with Mn/Pb molar feed ratios of (c) 2.0, (d) 5.0, and (e) 7.5, respectively. Insets show their PL photographs dispersed in cyclohexane under ultraviolet lamp irradiation. Reproduced with permission from ref. 52. Copyright 2017, American Chemical Society.

Moreover, due to the wide choice of solvents and ligands in this approach, the composition and morphologies of transition metal ion-doped cesium lead halide perovskite NCs can be readily manipulated. For instance, $CsPbBr_3$:$Mn^{2+}$ NCs and magic-sized clusters (MCS) with a size of 300 nm can be prepared based on the ligand of benzoic acid (BA) and benzylamine (BZA).[111] Specifically, $MnCl_2$ or $MnBr_2$ was dissolved in DMF containing BA and BAZ, with a [BA]/[Pb] ratio of 30. The DMF solution was then injected rapidly into toluene with vigorous stirring at a [DMF]/[toluene] volume ratio of 1 : 10. At a relatively low [BA]/[Pb] concentration ratio of 12, $CsPbBr_3$:$Mn^{2+}$ NCs with ~12 nm can be obtained. Nevertheless, the remaining small amount of DMF may be detrimental to $CsPbBr_3$:$Mn^{2+}$ NCs, because the $CsPbBr_3$:$Mn^{2+}$ NCs were unstable in DMF. In this regard, Xu *et al.* developed a

 

DMF-free method to obtain $CsPbCl_3$:$Mn^{2+}$ NCs. Toluene instead of DMF was used to dissolve CsAc, $Pb(Ac)_2$, $Mn(Ac)_2$ and ligands. After adding HCl into the toluene solution, $CsPbCl_3$ $Mn^{2+}$ NCs were precipitated.[112,113] Similarly, Pan *et al.* also reported the synthesis of $Ni^{2+}$-doped $CsPb(Cl/Br)_3$ NCs.[114]

# 3. Optical properties manipulation

Through the above-mentioned methods, transition metal ion-doped cesium lead halide perovskite NCs can be prepared, where their optical properties can be manipulated *via* changing the experimental conditions like reaction time, reaction temperature and concentration of the precursors. Specifically, the size, morphology and surface of the NCs may be readily tuned *via* the hot injection method.[115] In the ion exchange method, the composition of the samples obtained is adjustable while maintaining the morphology. As a result, the PL intensity, emission band or PL lifetime of the transition metal ion-doped cesium lead halide perovskite NCs can be manipulated.[116] In the supersaturated crystallization method, it is difficult to finely control the morphology due to the rapid precipitation. Consequently, the PL peak of the obtained products may be relatively broad.[52]

In this section, we will survey several typical strategies regarding the manipulation of optical properties of cesium lead halide perovskite NCs by doping them with transition metal ions, in order to improve their stabilities, enhance their luminescence efficiency, and tune their emission band or PL lifetime.

## 3.1. Improving stability

The applications of cesium lead halide perovskite NCs are severely limited by their poor intrinsic stabilities, which are mainly associated with the low formation energies of perovskite lattices.[117] Particularly, cesium lead halide perovskite NCs are prone to deteriorate when in contact with moisture in the air. Moreover, it was reported that heat, oxygen, ultraviolet (UV)-light irradiation, strong sunlight irradiation, and electronic field may accelerate this process.[118] These concerns greatly motivate the exploration of transition metal ion-doped cesium lead halide perovskite NCs, aiming to overcome the poor stability of cesium lead halide perovskite NCs.[119,120]

Among the $CsPbX_3$ (X = Cl, Br, or I) NCs, $CsPbI_3$ NCs exhibit the worst stability due to the large ion radius of the $I^-$ ion compared with $Br^-$ and $Cl^-$ ions.[119] It was proved that $I^-$ ions with a large radius may easily induce lattice distortion as well as phase transformation.[121] Furthermore, the crystal structural variation of $CsPbI_3$ NCs may significantly affect their PL properties. In particular, $CsPbI_3$ in cubic-phase ($\alpha$-$CsPbI_3$, $E_g$ = 1.73 eV) exhibiting excellent optical performance is prone to be transformed to an orthorhombic phase ($\delta$-$CsPbI_3$, $E_g$ = 2.25 eV) with the poor optical performance. Thus, it is critical to maintain the framework of a corner-sharing $[PbI_6]^{4-}$ octahedron in $\alpha$-$CsPbI_3$. Nevertheless, due to the ionic nature of the $CsPbI_3$ NC lattice, the surface halide vacancy would accelerate the breakdown of $CsPbI_3$ NCs. To overcome such an obstacle, several research groups doped small radius ions like $Mn^{2+}$, $Zn^{2+}$ or $Ni^{2+}$ in $CsPbI_3$ NCs to suppress the rotation of $[PbI_6]^{4-}$ octahedra by enhancing the energy barrier. Such cation doping induces lattice contractions and the Goldschmidt tolerance factor increments, thus making the $CsPbI_3$ NCs more stable in the cubic phase.[27] As a representative example, $CsPbI_3$:$Mn^{2+}$ still exhibited bright emissions after storage in toluene for more than 30 days, while the undoped $CsPbI_3$ counterparts exhibited weak emissions after several days.[58]

In addition to colloidal $CsPbX_3$ NCs, the stability of $CsPbX_3$ NCs-based films can also be substantially improved by doping with transition metal ions. When preparing $CsPbI_3$ NCs-based films, the loss of ligands during the washing process may result in iodine vacancy ($V_I$) defects, which would accelerate the phase transition process.[35] However, the formation energy of $V_I$ defects can be enhanced by transition metal ions doping, enabling the reduction of $V_I$ defects and inhibiting phase transition. It was reported that the PLQY of $CsPbI_3$:$Zn^{2+}$ films maintained 80% of its initial value after 10 days (Fig. 7a and b).[80] In contrast, the emission of pure $CsPbI_3$ films disappeared completely after 10 days. As shown in Fig. 7a, the optimal improvement of stability can be achieved with doping of 5 mol% $Zn^{2+}$ in $CsPbI_3$ NCs.

Compared with mono-halide $CsPbX_3$ NCs mentioned above, mixed halide $CsPbX_3$ NCs such as $CsPb(Br/Cl)_3$ and $CsPb(Br/I)_3$ NCs suffer from severe problems of halogen segregation. To solve this issue, $Cu^{2+}$ ions with a relatively small radius (0.72 Å) were proposed to partly replace $Pb^{2+}$ ions in the lattice of $CsPbBrI_2$ NCs, in order to enhance the bond strength of Pb-halides and suppress the halogen segregation (Fig. 7c).[122] Specifically, the emission color of pristine $CsPb(Br/I)_3$ NC-based films gradually changed from red to green after 2 days, which originated from the halogen segregation of $CsPb(Br/I)_3$ NCs into $\alpha$-$CsPbI_3$, $\delta$-$CsPbI_3$ and $CsPbBr_3$ NCs. Nevertheless, $CsPbBrI_2$:$Cu^{2+}$ NCs maintained bright red luminescence for more than 15 days.

To shed more light on the mechanism of ionic migration suppression of mixed halide $CsPbX_3$ NCs by transition metal doping, Chen *et al.* investigated lattice stabilization in $CsPb(Br/I)_3$ NCs by doping with $Ni^{2+}$ ions.[77] For pristine $CsPb(Br/I)_3$ NCs, the PL spectra evolved from one peak (587 nm) to three peaks (610 nm, 521 nm, and 667 nm) after 300 min, and the emission color changed from red to white. With the incorporation of $Ni^{2+}$ in $CsPbBr_{1.5}I_{1.5}$, such emission color variability was greatly inhibited as shown in the Commission Internationale de l'Eclairage (CIE) 1931 chromaticity diagram (Fig. 7d), indicative of the effective improvement of photostability. To reveal the mechanism, they illustrated $CsPbBr_3$:$Ni^{2+}$ as a model. Accordingly, ion migration in $CsPbBr_3$ can be described by a series exchange of $Br^-$ with neighboring bromide vacancy ($V_{Br}$), which were marked as P1, P2 and P3. After $Ni^{2+}$ doping, the transition states of $V_{Br}$ hopping from P1 to P2 and from P2 to P3 were determined to be 0.318 eV and 0.408 eV, respectively, both of which are higher than the value (0.26 eV) in pure $CsPbBr_3$. Correspondingly, $V_{Br}$ hopping toward $Ni^{2+}$ ion was forbidden in energy, resulting in a repulsion effect on the migrating $V_{Br}$ and reducing the $V_{Br}$ migration channels. Consequently, the $V_{Br}$

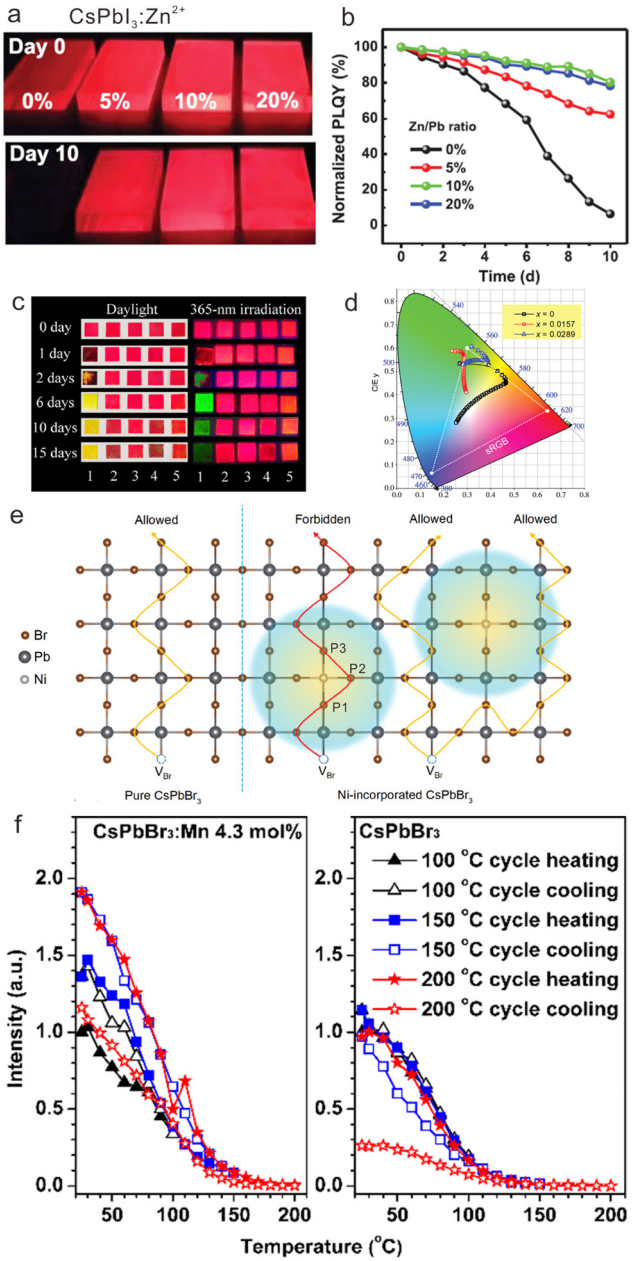


Fig. 7 (a) PL photographs and (b) normalized PLQYs for α-phase $CsPbI_3$ and $CsPbI_3$:$Zn^{2+}$ NCs films as a function of aged days. (c) PL photographs of $Cu^{2+}$-doped $CsPb(Br/I)_3$ NCs under UV illumination during 15 days. (d) CIE 1931 chromaticity diagram for $CsPb_{1-x}Ni_xBr_{1.5}I_{1.5}$ with different $x$ values upon different measurement time from 0 to 300 min. (e) Schematic illustration of the repelling effect of $Ni^{2+}$ on the moving $V_{Br}$. Compared with pure $CsPbBr_3$, the repelling effect reduces the ionic migration channels and lengthens the migration path. (f) Temperature-dependent PL intensities for excitonic luminescence of $CsPbBr_3$:$Mn^{2+}$ (4.3 mol%) and pure $CsPbBr_3$ NCs *via* three heating/cooling cycles at 100, 150, and 200 °C, respectively. (a) and (b) Reproduced with permission from ref. 80. Copyright 2021, Wiley-VCH Verlag GmbH l Co. KGaA, Weinheim; (c) reproduced with permission from ref. 105. Copyright 2019, Elsevier; (d) and (e) reproduced with permission ref. 77. Copyright 2022, Wiley-VCH Verlag GmbH l Co. KGaA, Weinheim; (f) reproduced with permission ref. 39. Copyright 2017, American Chemical Society.

migration length in $CsPbBr_3$ was increased after $Ni^{2+}$ doping, leading to long-range lattice stabilization (Fig. 7e). They systematically compared $Ni^{2+}$ with $Zn^{2+}$ and $Bi^{3+}$ for the ionic migration suppression effect, which indicated that the coupling between partially filled 3d orbital of $Ni^{2+}$ and Pb 6s-Br 4p antibonding states is the key to lattice stabilization. Such coupling can passivate the active Pb $6s^2$ lone-pair electron and enhance the chemical bond strength in surrounding Pb-Br octahedra, thus facilitating long-range lattice stabilization.

Because of the intrinsically low formation energies of perovskite lattices, the thermal stability of cesium lead halide perovskite NCs is another critical issue that needs to be addressed. Doping with transition metal ions may effectively engineer the local structure of cesium lead halide perovskite NCs, which improves their thermal stability by enhancing the formation energies of perovskite lattices. For instance, we doped $Mn^{2+}$ in $CsPbBr_3$ NCs, which displayed better thermal stability relative to the pristine $CsPbBr_3$ counterparts.[39] We compared the temperature-dependent PL spectra of pristine $CsPbBr_3$ and $CsPbBr_3$:$Mn^{2+}$ NCs by gradually heating them from 25 °C to higher temperatures (100, 150, and 200 °C) and then cooling them to 25 °C. Subsequently, the PL spectra at 25 °C were monitored (Fig. 7f and g). It was found that the room-temperature PL intensities for $CsPbBr_3$:$Mn^{2+}$ can retain about 120% of their initial intensities undergoing three heating and cooling cycles at 100, 150, and 200 °C, which is superior to their undoped counterparts. Hitherto, the enhancement in thermal stability has also been achieved in $Mn^{2+}$-doped $CsPbCl_3$ NCs, $Cd^{2+}$, $Co^{2+}$ or $Zn^{2+}$-doped $CsPbBr_3$ NCs, and $Ni^{2+}$, $Zn^{2+}$, or $Mn^{2+}$ doped $CsPbI_3$ NCs, respectively.[35,76,109,123,124]

Note that the thermal stability of cesium lead halide perovskite NCs was closely associated with defect or trap states. To this regard, $Ni^{2+}$ doping was proposed, which was demonstrated to reduce the defect or trap states of $CsPbCl_3$ NCs to improve their thermal stability.[125] After $Ni^{2+}$ doping, the thermal activation energy was increased from 58.7 meV to 82.6 meV, which effectively alleviated the thermal quenching of $CsPbCl_3$ NCs. Correspondingly, the thermal quenching temperature was improved from 280 K for $CsPbCl_3$ NCs to 360 K for $CsPbCl_3$:$Ni^{2+}$ NCs.

### 3.2. Enhancing luminescence efficiency

The development of cesium lead halide perovskite NCs with excellent luminescence efficiency is a key prerequisite for their practical applications. However, small-sized $CsPbX_3$ NCs often suffer from low PLQYs. Thus, enhancing the luminescence efficiency of cesium lead halide perovskite NCs is an important goal in promoting their fundamental research and applications. Several studies have revealed that doping with transition metal ions may surmount this problem through tuning of near-band edge states or local structures. Hitherto, a series of transition metal ions including $Ni^{2+}$, $Mn^{2+}$, $Cu^{2+}$, and $Zn^{2+}$ have been widely explored to improve the PLQY of $CsPbX_3$ NCs at different spectral regions, such as $CsPbCl_3$:$Ni^{2+}$,$Pr^{3+}$ NCs with near-infrared (NIR) emission, $CsPbI_3$:$Zn^{2+}$ with deep-red emission, $CsPbCl_3$:$Ni^{2+}$,$Mn^{2+}$,$Zn^{2+}$ NCs with red emission, $CsPbBr_3$:$Zn^{2+}$

 

with green emission, $CsPbBr_{1-x}Cl_x:Cu^{2+}$ NCs and $CsPbBr_{1-x}Cl_x:Mn^{2+}$ NCs with blue emission, and $CsPbCl_3:Zn^{2+}$ with violet emission.[23,35,37,79,83,126–130]

Compared with $CsPbBr_3$ NCs, the PLQYs of $CsPbCl_3$ and $CsPbI_3$ NCs are relatively low.[36] Benefiting from the suppression of defect states by doping with transition metal ions, the PLQY of $CsPbI_3$ NCs can be effectively improved, as revealed by Li *et al.* through $Zn^{2+}$ doping.[36] In their work, zinc non-halide compounds including zinc acetylacetonate ($Zn(acac)_2$), zinc acetate ($ZnAc_2$) or zinc stearate (ZnSt) were employed as precursors for doping of $Zn^{2+}$ in $CsPbI_3$ NCs. The as-prepared $Zn^{2+}$-doped $CsPbI_3$ NCs displayed stronger red emission than the undoped $CsPbI_3$ NCs, owing to the increased electron–hole radiative recombination after $Zn^{2+}$ doping. Specifically, $CsPbI_3:Zn^{2+}$ prepared from $Zn(acac)_2$ exhibited a PLQY as high as 76%, which was 120% enhancement relative to that of the undoped $CsPbI_3$ counterparts (Fig. 8a and b). On the basis of the absorption spectra, PL decays, and space-charge-limited current measurements for pristine and $Zn^{2+}$-doped $CsPbI_3$ NCs, it was confirmed the density of the localized defect states near the band edge decreased after $Zn^{2+}$ doping, thus effectively inhibited nonradiative recombination rate and enhanced the PLQY of $CsPbI_3$ NCs (Fig. 8c and d).

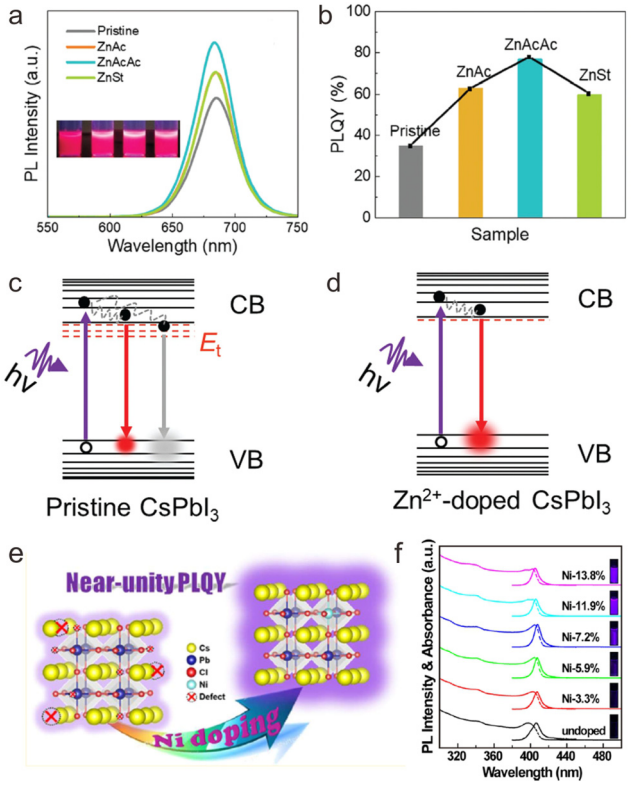


Fig. 8 (a) PL spectra of pristine and $Zn^{2+}$-doped $CsPbI_3$ NCs and their PL photographs under UV lamps. (b) PLQYs of pristine and $Zn^{2+}$-doped $CsPbI_3$ NCs. Schematic illustration of radiative and nonradiative recombination of $CsPbI_3$ NCs (c) before and (d) after $Zn^{2+}$ doping. CB and VB refer to conduction band and valence band respectively. (e) Schematic illustration of $Ni^{2+}$ doping in $CsPbCl_3$ NCs to achieve near-unity PLQY. (f) Absorption and PL spectra of undoped and $Ni^{2+}$ doped $CsPbCl_3$ NCs. Insets show the photographs of NC solution under UV (365 nm) illumination. (a)–(d) Reproduced with permission from ref. 36. Copyright 2020, Royal Society of Chemistry (United Kingdom); (e) and (f) reproduced with permission from ref. 78. Copyright 2018, American Chemical Society.

Moreover, transition metal dopants may improve the PLQY of cesium lead halide perovskite NCs by tuning the population of band edge states. For example, $Ti^{3+}$ ions were demonstrated to introduce more band edge states around the conduction band minimum of $CsPbCl_3$, favoring the release of electrons into the conduction band.[74] As a result, the PLQY of $CsPbCl_3$ was markedly improved from 0.08% to 48.4%. In another work, Wu *et al.* proposed that the transition from the $T_2$ energy level of $Cu^{2+}$ to the conduction band of $CsPb(Cl/Br)_3$ NCs promoted the recombination of excitons *via* the radiative pathway, thus effectively enhancing the PLQYs of $CsPbCl_3$ NCs from 3% to 51%.[82]

In addition to near band edge states tuning, the doping with transition metal ions may also engineer the local structure of cesium lead halide perovskite NCs to improve their luminescence efficiency. A typical example is $Ni^{2+}$ doping in $CsPbCl_3$ NCs, where $NiCl_2$ was employed as a dopant precursor.[78] As a result, the PLQY of $CsPbCl_3$ NCs can be increased from 2.4% to 96.5% (Fig. 8e and f). It was confirmed that doping of $Ni^{2+}$ ions substantially removed the structural defects of $V_{Cl}$, resulting in improved short-range order of the perovskite lattice. Similarly, De *et al.* reported that $Cu^{+}$ doping may increase the PLQY of $CsPbCl_3$ NCs from 0.5% to 60%.[75] They attributed the significant PLQY enhancement to the rectifying octahedral distortion of the crystal and the passivation of $V_{Cl}$ on the surface.

Furthermore, doping with transition metal ions can be utilized to strengthen the quantum confinement effect through engineering the local structure of cesium lead halide perovskite NCs, thus improving their luminescence efficiency. It was demonstrated that $Mn^{2+}$ doping with a molar concentration of 3 mol% in $CsPbCl_3$ NCs significantly increased their PLQY from 0.5% to 26%, due to the formation of a Ruddlesden–Popper structure in $CsPbCl_3$ NCs.[131] In these $CsPbCl_3:Mn^{2+}$ NCs, the excitons were confined to the subdomains separated by the Ruddlesden–Popper structure. Such quantum confinement favored the enhancement of the exciton oscillator strength, which contributed to the prominent exciton resonance in $CsPbCl_3:Mn^{2+}$ NCs, thus enhancing the excitonic emission.

### 3.3. Tuning emission band

Since the valence band maximum (VBM) of cesium lead halide perovskites is formed by the mixing of halide p-orbitals and metal s-orbitals, the change of composition and crystal structure by doping with transition metal ion may affect their bandgap ($E_g$) as well as the luminescence emission band.[132,133] In addition, several transition metal ion dopants can serve as activators in cesium lead halide perovskite NCs to donate new emission bands.

In $CsPbX_3$ NCs, it was reported that replacing $Pb^{2+}$ ($r$ = 119 pm) with smaller transition metal ions such as $Cd^{2+}$ ($r$ = 95 pm), or $Zn^{2+}$ ($r$ = 74 pm) led to blue shifting of the emission band due to the lattice contraction. Specifically, $CsPbBr_3:Cd^{2+}$ and $CsPbBr_3:Zn^{2+}$ NCs exhibited blue emissions, which are 50–60 nm blue-shifted

relative to the green-emitting $CsPbBr_3$ NCs.[99,134,135] Similarly, the PL peak of $CsPbI_3$ NCs was tuned from 690 nm to 676 nm after doping of $Zn^{2+}$ ions.[35]

Recently, we proposed a facile strategy to design efficient UV-emitting cesium lead halide perovskites by engineering the $E_g$ of $CsPbCl_3$ NCs.[89] Benefiting from the doping of $Cd^{2+}$ in $CsPbCl_3$ NCs, we demonstrated that their bandgap can be tuned from the visible region into the UV region with the emission peak at 381 nm (Fig. 9a and b). $Cd^{2+}$ doping induced lattice contraction as confirmed by XRD patterns. According to theoretical calculations based on density functional theory, the $Cd^{2+}$ orbital caused little changes in the orbital composition near the Fermi level. Nevertheless, $Cd^{2+}$ doping increased the bonding interactions between the Cd-5s and Cl-3p states, resulting in the broadening of $E_g$ (Fig. 9c).

Another common strategy for emission band tuning of cesium lead halide perovskite NCs is the introduction of new activators. Several transition metal ion dopants (*e.g.*, $Mn^{2+}$, $Cd^{2+}$) frequently acted as activators in various hosts. Thus, they can donate new emission bands to cesium lead halide perovskite NCs.[23,90,91] For example, $CsPbCl_3$ NCs usually exhibit violet emission. It was reported that $Cd^{2+}$ endowed $CsPbCl_3$ NCs with yellow or red emissions.[72] The new emission band peaking at 600 nm was assigned to the transition from $^3E_g$ to the ground state ($^1A_{1g}$) of $[CdCl_6]^{4-}$.

$Mn^{2+}$ is another frequently utilized activator in various hosts. In $CsPbCl_3$:$Mn^{2+}$ NCs, we observed a new emission band belonging to $^4T_1 \rightarrow {}^6A_1$ of $Mn^{2+}$ (Fig. 10a).[39] Through tuning the $Mn^{2+}$ feeding concentration from 0 to 60 mol%, the PL color of the $CsPbCl_3$:$Mn^{2+}$ solution can be tuned from purple to yellow due to the change in PL intensity ratio of $CsPbCl_3$ and $Mn^{2+}$ (Fig. 10b and c). The PL peak of $Mn^{2+}$ shifted from 570 nm to 625 nm as a result of crystal field variation with increasing $Mn^{2+}$ concentration. According to the excitation spectra, we confirmed that the strong PL emission of $Mn^{2+}$ originated from the efficient energy transfer from the exciton of $CsPbCl_3$ to $Mn^{2+}$ dopants (Fig. 10d). Similarly, energy transfer from exciton to $Mn^{2+}$ dopants was achieved in $CsPbCl_xBr_{3-x}$:$Mn^{2+}$ NCs.[23] With increasing the content of $Cl^-$ in $CsPbCl_xBr_{3-x}$:$Mn^{2+}$ NCs, the emission of $Mn^{2+}$ became stronger due to the increased energy transfer efficiency from the $CsPbCl_xBr_{3-x}$ host to $Mn^{2+}$ ions.

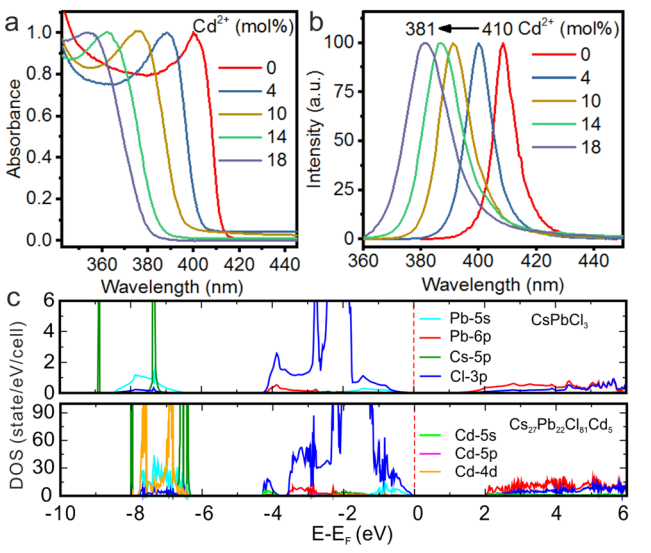


Fig. 9 (a) Absorption and (b) PL spectra for the pure $CsPbCl_3$ and $CsPbCl_3$:$Cd^{2+}$ NCs. (c) Calculated density of states for pure $CsPbCl_3$ and $CsPbCl_3$:$Cd^{2+}$. Reproduced with permission from ref. 89. Copyright 2021, Wiley-VCH Verlag GmbH l Co. KGaA, Weinheim.

### 3.4. Manipulating PL lifetime

The PL lifetimes of excitonic emission for transition metal ion-doped cesium lead halide perovskite NCs are usually several to hundreds of nanoseconds. The PL lifetime ($\tau_{PL}$), which is related to radiative (r) and nonradiative (nr) processes, can be depicted as $1/\tau_{PL} = 1/\tau_r + 1/\tau_{nr}$.[89] In most cases, doping transition metal ions into cesium lead halide perovskite NCs may induce more defect states and increase the nonradiative recombination rate ($1/\tau_{nr}$). Correspondingly, the PL lifetime of excitonic emission would be shortened. For instance, we found that the nonradiative recombination rate ($1/\tau_{nr}$) in $CsPbCl_3$ NCs significantly increased from 0.078 to 0.693 $\mu s^{-1}$ after doping of $Cd^{2+}$.[89] As such, the PL lifetime of $CsPbCl_3$ NCs decreased from 5.63 to 1.43 ns after $Cd^{2+}$ doping. Similarly, it was reported that the PL lifetime of $CsPbI_3$ NCs decreased from 215.2 ns to 85.0 ns by doping $Zn^{2+}$.[35]

By contrast, it was discovered that several transition metal ions doping may suppress the intrinsic defects of cesium lead halide perovskite NCs, thereby prolonging their PL lifetimes.[28,75,135–137] Sun *et al.* observed that the PL lifetime of $CsPbCl_3$ NCs was markedly increased from 2.58 to 18.39 ns after doping of $Ni^{2+}$.[78] $Ni^{2+}$ doping substantially eliminated the intrinsic defects of $Cl^-$ vacancies in the $CsPbCl_3$ NCs, resulting in increased short-range order of the lattice. Therefore, $Ni^{2+}$ doped $CsPbCl_3$ NCs exhibited increased defect formation energy and longer PL lifetime than the undoped counterparts.

Furthermore, researchers prolonged the PL lifetime of cesium lead halide perovskite NCs from nanoseconds to microseconds by virtue of the long-lived energy level of transition metal ions. Pradeep *et al.* proposed a concept of vibrationally assisted delayed fluorescence (VADF) in $CsPbCl_xBr_{3-x}$:$Mn^{2+}$ NCs to harvest delayed fluorescence of $Mn^{2+}$.[138] The excited state electrons of $CsPb(Cl/Br)_3$:$Mn^{2+}$ NCs can be conserved for several microseconds to milliseconds within the excited-state energy levels of $Mn^{2+}$. With vibrational assistance, electrons were transferred from the excited-state energy level of $Mn^{2+}$ to the $CsPb(Cl/Br)_3$ host to obtain the VADF (Fig. 11a). Such energy transfer from $Mn^{2+}$ to the $CsPb(Cl/Br)_3$ host was significantly affected by vibrational coupling, which was closely related to phonon band structure and temperature (Fig. 11b). To be specific, in $CsPb(Cl/Br)_3$:$Mn^{2+}$ NCs with small $E_g$ such as $CsPbBr_3$:$Mn^{2+}$ and $CsPb(Cl_{0.2}/Br_{0.8})_3$:$Mn^{2+}$ NCs, substantial gated excitonic emission along with the $Mn^{2+}$ emission can be observed at 300 K after a delay of 150 μs (Fig. 11c). Nevertheless, it was demonstrated that the energy level of $Mn^{2+}$ situated deeper in the conductive band of $CsPb(Cl/Br)_3$ with larger $E_g$

 

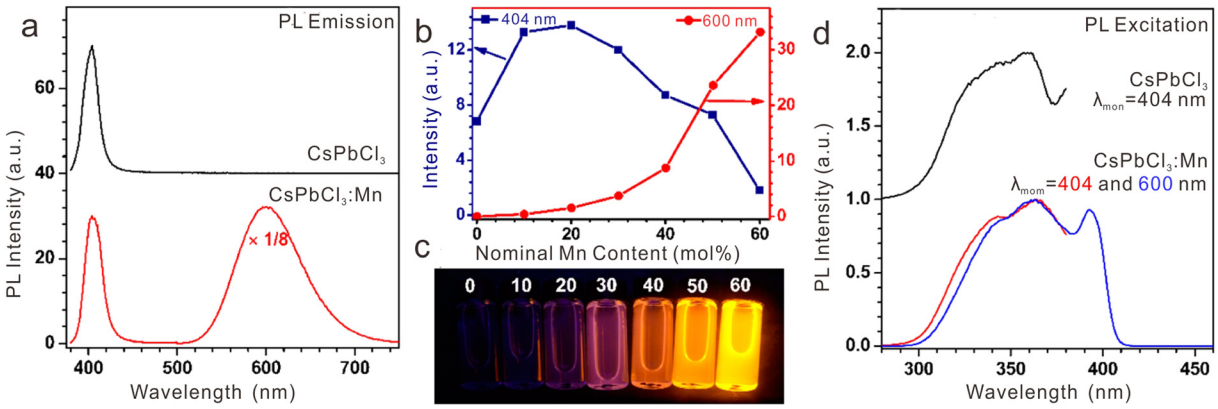


Fig. 10 (a) PL emission spectra for pure $CsPbCl_3$ and $Mn^{2+}$-doped $CsPbCl_3$ NCs upon UV excitation at 362 nm. (b) PL intensities for excitonic or $Mn^{2+}$-related emissions of $CsPbCl_3$:$Mn^{2+}$ NCs centered at 404 and 600 nm as a function of the feed doping concentration of $Mn^{2+}$ ions from 0 to 60 mol%, and (c) their corresponding PL photographs in cyclohexane solution under 362 nm UV lamp irradiation. (d) Comparison of PL excitation spectra for pure $CsPbCl_3$ and $Mn^{2+}$-doped $CsPbCl_3$ NCs by monitoring the emissions at 404 nm and 600 nm, respectively. Reproduced with permission from ref. 39. Copyright 2017, American Chemical Society.

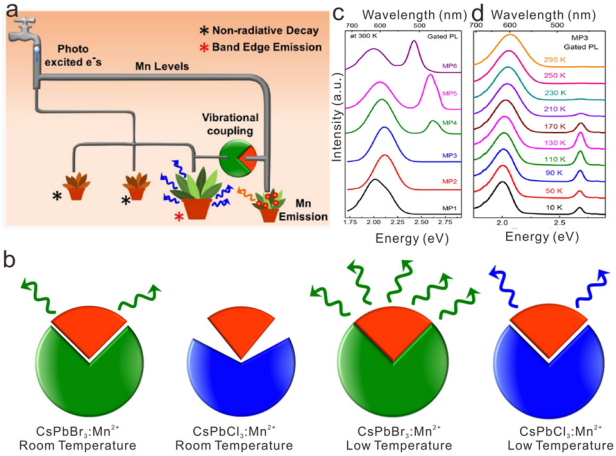


Fig. 11 (a) Schematic illustration of vibrationally assisted delayed fluorescence of $CsPb(Cl/Br)_3$:$Mn^{2+}$ NCs. (b) Schematic illustration of phonon coupling for $Mn^{2+}$-doped $CsPbBr_3$, and $CsPbCl_3$ perovskite NCs. (c) Room-temperature gated PL emission for $CsPb(Cl/Br)_3$:$Mn^{2+}$ perovskite NCs (MP1–MP6 stand for the $CsPb(Cl/Br)_3$:$Mn^{2+}$ with Br content of 0, 20%, 40%, 60%, 80% and 100%). (d) Temperature-dependent gated PL emission for $CsPb(Cl/Br)_3$:$Mn^{2+}$ NCs. Reproduced with permission from ref. 138. Copyright 2019, American Chemical Society.

(*e.g.*, $CsPb(Cl_{0.6}/Br_{0.4})_3$:$Mn^{2+}$ and $CsPbCl_3$:$Mn^{2+}$NCs), thus making energy transfer assisted by vibrational coupling much harder. Since low temperature may strengthen the coupling, leading to more efficient energy transfer, $CsPb(Cl_{0.6}/Br_{0.4})_3$:$Mn^{2+}$ and $CsPbCl_3$:$Mn^{2+}$NCs with large $E_g$ only exhibited the gated PL of excitons below 170 K (Fig. 11d).

## 4. Conclusion and prospects

During the past decade, doping cesium lead halide perovskite NCs with transition metal ions has been demonstrated to be a robust strategy for engineering their structural, morphological, and optoelectronic properties. With the rapid development of advanced synthesis techniques, significant progress has been made in tackling the problems of controlled synthesis of transition metal ion-doped cesium lead halide perovskite NCs. The unique optical properties of transition metal ion-doped cesium lead halide perovskite NCs bestow great potential for the exploitation of high-performance luminescent materials and novel optoelectronic devices. Despite these achievements, there are still several challenges to be solved to fully exploit the potential of transition metal ion-doped cesium lead halide perovskite NCs, which would undoubtedly accelerate their commercialization.

First, due to the ionic crystal nature and the high reactivity of the halide anions in the cesium lead halide perovskite NCs, the nucleation and growth process of cesium lead halide perovskite NCs is fast and uncontrollable. As such, it is essential to precisely regulate the crystallization kinetics of cesium lead halide perovskite NCs, as well as the doping content of transition metal ions. To circumvent the shortcomings of conventional approaches for the fast reaction of preparing cesium lead halide perovskite NCs, novel strategies like vacuum evaporation or light-triggered synthesis may be the smart choice. For example, the ion migration, doping content and composition can be readily controlled in light-triggered synthesis by adjusting either the photon dose or the wavelength of the excitation light.

Second, a comprehensive investigation of the microstructure of transition metal ions in the perovskite hosts is a prerequisite for exploring novel kinds of transition metal ion-doped cesium lead halide perovskite NCs and rationally modulating their optical properties. Especially, low-dimensional cesium lead halide perovskite NCs (*e.g.*, 0D $Cs_4PbX_6$ and 2D $CsPb_2X_5$) exhibit better environmental stability and higher PLQYs in solid powders than their 3D counterparts. The energy transfer and local electronic structure should be clearly deciphered *via* fundamental photophysical studies and theoretical calculations, which may contribute to rationally optimizing the luminescent properties of transition metal ion-doped cesium lead halide perovskite NCs.

Last but not least, the studies on cesium lead halide perovskite NCs are mainly restricted to the visible spectral region. Cesium lead halide perovskite NCs with UV/NIR light emission *via* transition metal ion doping still suffer from weak emissions intensities or poor stabilities, due to the inevitable defects formed during their crystal growth. Thus, it is highly desirable to develop versatile strategies for engineering the local and surface structure of cesium lead halide perovskite NCs to achieve highly efficient UV/NIR-emitting materials for diverse applications.

## Conflicts of interest

There are no conflicts to declare.

## Acknowledgements

This work was financially supported by the National Key R&D Program of China (No. 2022YFB3503700), the National Natural Science Foundation of China (No. 21975257, 22275188, 22135008, U22A20398), the CAS/SAFEA International Partnership Program for Creative Research Teams, Natural Science Foundation of Fujian Province (No. 2021L3024) and the China Postdoctoral Science Foundation (No. 2021M703219).

## References

1 L. Protesescu, S. Yakunin, M. I. Bodnarchuk, F. Krieg, R. Caputo, C. H. Hendon, R. X. Yang, A. Walsh and M. V. Kovalenko, Nanocrystals of Cesium Lead Halide Perovskites ($CsPbX_3$, X = Cl, Br, and I): Novel Optoelectronic Materials Showing Bright Emission with Wide Color Gamut, *Nano Lett.*, 2015, **15**, 3692–3696.

2 J. Z. Ye, M. M. Byranvand, C. O. Martnez, R. L. Z. Hoye, M. Saliba and L. Polavarapu, Defect Passivation in Lead-Halide Perovskite Nanocrystals and Thin Films: Toward Efficient LEDs and Solar cells, *Angew. Chem., Int. Ed.*, 2021, **60**, 21636–21660.

3 Y. H. Zhang, R. J. Sun, X. Y. Qi, K. F. Fu, Q. S. Chen, Y. C. Ding, L. J. Xu, L. M. Liu, Y. Han, A. V. Malko, X. G. Liu, H. H. Yang, O. M. Bakr, H. Liu and O. F. Mohammed, Metal Halide Perovskite Nanosheet for X-ray High-Resolution Scintillation Imaging Screens, *ACS Nano*, 2019, **13**, 2520–2525.

4 Q. Chen, J. Wu, X. Ou, B. Huang, J. Almutlaq, A. A. Zhumekenov, X. Guan, S. Han, L. Liang, Z. Yi, J. Li, X. Xie, Y. Wang, Y. Li, D. Fan, D. B. L. Teh, A. H. All, O. F. Mohammed, O. M. Bakr, T. Wu, M. Bettinelli, H. Yang, W. Huang and X. Liu, All-inorganic perovskite nanocrystal scintillators, *Nature*, 2018, **561**, 88–93.

5 A. K. Jena, A. Kulkarni and T. Miyasaka, Halide Perovskite Photovoltaics: Background, Status, and Future Prospects, *Chem. Rev.*, 2019, **119**, 3036–3103.

6 X. Y. Zhang, L. N. Li, Z. H. Sun and J. H. Luo, Rational chemical doping of metal halide perovskites, *Chem. Soc. Rev.*, 2019, **48**, 517–539.

7 D. Yang, X. Li, W. Zhou, S. Zhang and H. Zeng, $CsPbBr_3$ Quantum Dots 2.0: Benzenesulfonic Acid Equivalent Ligand Awakens Complete Purification, *Adv. Mater.*, 2019, **31**, 1900767.

8 H. Huang, B. Chen, Z. Wang, T. F. Hung, A. S. Susha, H. Zhong and A. L. Rogach, Water resistant $CsPbX_3$ nanocrystals coated with polyhedral oligomeric silsesquioxane and their use as solid state luminophores in all-perovskite white light-emitting devices, *Chem. Sci.*, 2016, **7**, 5699–5703.

9 D. Yang, X. Li, Y. Wu, C. Wei, Z. Qin, C. Zhang, Z. Sun, Y. Li, Y. Wang and H. Zeng, Surface Halogen Compensation for Robust Performance Enhancements of $CsPbX_3$ Perovskite Quantum Dots, *Adv. Opt. Mater.*, 2019, **7**, 1900276.

10 J. J. Wei, W. Zheng, P. Huang, Z. L. Gong, Y. Liu, S. Lu, Z. Li and X. Y. Chen, Direct photoinduced synthesis of lead halide perovskite nanocrystals and nanocomposites, *Nano Today*, 2021, **39**, 101179.

11 J. S. Yao, J. Ge, B. N. Han, K. H. Wang, H. B. Yao, H. L. Yu, J. H. Li, B. S. Zhu, J. Z. Song, C. Chen, Q. Zhang, H. B. Zeng, Y. Luo and S. H. Yu, $Ce^{3+}$-Doping to Modulate Photoluminescence Kinetics for Efficient $CsPbBr_3$ Nanocrystals Based Light-Emitting Diodes, *J. Am. Chem. Soc.*, 2018, **140**, 3626–3634.

12 H. Huang, R. Li, S. Jin, Z. Li, P. Huang, J. Hong, S. Du, W. Zheng, X. Chen and D. Chen, Ytterbium-Doped $CsPbCl_3$ Quantum Cutters for Near-Infrared Light-Emitting Diodes, *ACS Appl. Mater. Interfaces*, 2021, **13**, 34561–34571.

13 D. Q. Chen, S. Zhou, F. F. Tian, H. T. Ke, N. Z. Jiang, S. J. Wang, Y. Z. Peng and Y. Liu, Halogen-Hot-Injection Synthesis of Mn-Doped $CsPb(Cl/Br)_3$ Nanocrystals with Blue/Orange Dual-Color Luminescence and High Photoluminescence Quantum Yield, *Adv. Opt. Mater.*, 2019, **7**, 1901082.

14 M. L. Liu, N. Z. Jiang, H. Huang, J. D. Lin, F. Huang, Y. P. Zheng and D. Q. Chen, $Ni^{2+}$-doped $CsPbI_3$ perovskite nanocrystals with near-unity photoluminescence quantum yield and superior structure stability for red light-emitting devices, *Chem. Eng. J.*, 2021, **413**, 127547.

15 D. X. Yang and D. X. Huo, Cation doping and strain engineering of $CsPbBr_3$-based perovskite light emitting diodes, *J. Mater. Chem. C*, 2020, **8**, 6640–6653.

16 N. Pradhan, Mn-Doped Semiconductor Nanocrystals: 25 Years and Beyond, *J. Phys. Chem. Lett.*, 2019, **10**, 2574–2577.

17 H. Kim, S. R. Bae, T. H. Lee, H. Lee, H. Kang, S. Park, H. W. Jang and S. Y. Kim, Enhanced Optical Properties and Stability of $CsPbBr_3$ Nanocrystals Through Nickel Doping, *Adv. Funct. Mater.*, 2021, **31**, 2102770.

18 B. Su, G. Zhou, J. Huang, E. Song, A. Nag and Z. Xia, $Mn^{2+}$-Doped Metal Halide Perovskites: Structure, Photoluminescence, and Application, *Laser Photon. Rev.*, 2020, **15**, 2000334.

19 Y. M. Chen, Y. S. Liu and M. C. Hong, Cation-doping matters in caesium lead halide perovskite nanocrystals: from physicochemical fundamentals to optoelectronic applications, *Nanoscale*, 2020, **12**, 12228–12248.

20 Y. H. Kye, C. J. Yu, C. H. Kim, Y. S. Kim and U. G. Jong, Influence of Metal-Ion Replacement on the Phase

 

Stabilization of Cubic All-Inorganic Cesium Lead Halide Perovskites: an Ab Initio Thermodynamic Formalism for Solution-Processed Cation Doping, *J. Phys. Chem. C*, 2021, **125**, 13195–13211.

21 Y. C. Chen, H. L. Chou, J. C. Lin, Y. C. Lee, C. W. Pao, J. L. Chen, C. C. Chang, R. Y. Chi, T. R. Kuo, C. W. Lu and D. Y. Wang, Enhanced Luminescence and Stability of Cesium Lead Halide Perovskite $CsPbX_3$ Nanocrystals by $Cu^{2+}$-Assisted Anion Exchange Reactions, *J. Phys. Chem. C*, 2019, **123**, 2353–2360.

22 Y. J. Guo, J. Su, L. Wang, Z. H. Lin, Y. Hao and J. J. Chang, Improved Doping and Optoelectronic Properties of Zn-Doped $CsPbBr_3$ Perovskite through Mn Codoping Approach, *J. Phys. Chem. Lett.*, 2021, **12**, 3393–3400.

23 Y. Z. Zheng, X. Yuan, J. Yang, Q. Y. Li, X. X. Yang, Y. Fan, H. B. Li, H. L. Liu and J. L. Zhao, Cu doping-enhanced emission efficiency of $Mn^{2+}$ in cesium lead halide perovskite nanocrystals for efficient white light-emitting diodes, *J. Lumin.*, 2020, **227**, 117586.

24 D. Ghosh, M. Y. Ali, A. Ghosh, A. Mandal and S. Bhattacharyya, Heterovalent Substitution in Mixed Halide Perovskite Quantum Dots for Improved and Stable Photovoltaic Performance, *J. Phys. Chem. C*, 2021, **125**, 5485–5493.

25 Y. B. Chen, H. W. Yang, J. Song and B. Zhang, An effective Fe(II) doping strategy for stable and highly photoluminescent $CsPbBrI_2$ nanocrystals, *J. Mater. Chem. C*, 2022, **10**, 5147–5154.

26 M. Lu, X. Y. Zhang, X. Bai, H. Wu, X. Y. Shen, Y. Zhang, W. Zhang, W. T. Zheng, H. W. Song, W. W. Yu and A. L. Rogach, Spontaneous Silver Doping and Surface Passivation of $CsPbI_3$ Perovskite Active Layer Enable Light-Emitting Devices with an External Quantum Efficiency of 11.2%, *ACS Energy Lett.*, 2018, **3**, 1571–1577.

27 A. Swarnkar, W. J. Mir and A. Nag, Can B-Site Doping or Alloying Improve Thermal- and Phase-Stability of All-Inorganic $CsPbX_3$ (X = CI, Br, I) Perovskites?, *ACS Energy Lett.*, 2018, **3**, 286–289.

28 A. Dey, J. Z. Ye, A. De, E. Debroye, S. K. Ha, E. Bladt, A. S. Kshirsagar, Z. Y. Wang, J. Yin, Y. Wang, L. N. Quan, F. Yan, M. Y. Gao, X. M. Li, J. Shamsi, T. Debnath, M. H. Cao, M. A. Scheel, S. Kumar, J. A. Steele, M. Gerhard, L. Chouhan, K. Xu, X. G. Wu, Y. X. Li, Y. N. Zhang, A. Dutta, C. Han, I. Vincon, A. L. Rogach, A. Nag, A. Samanta, B. A. Korgel, C. J. Shih, D. R. Gamelin, D. H. Son, H. B. Zeng, H. Z. Zhong, H. D. Sun, H. V. Demir, I. G. Scheblykin, I. Mora-Sero, J. K. Stolarczyk, J. Z. Zhang, J. Feldmann, J. Hofkens, J. M. Luther, J. Perez-Prieto, L. Li, L. Manna, M. I. Bodnarchuk, M. V. Kovalenko, M. B. J. Roeffaers, N. Pradhan, O. F. Mohammed, O. M. Bakr, P. D. Yang, P. Muller-Buschbaum, P. V. Kamat, Q. L. Bao, Q. Zhang, R. Krahne, R. E. Galian, S. D. Stranks, S. Bals, V. Biju, W. A. Tisdale, Y. Yan, R. L. Z. Hoye and L. Polavarapu, State of the Art and Prospects for Halide Perovskite Nanocrystals, *ACS Nano*, 2021, **15**, 10775–10981.

29 A. R. Kirmani, J. M. Luther, M. Abolhasani and A. Amassian, Colloidal Quantum Dot Photovoltaics: Current Progress and Path to Gigawatt Scale Enabled by Smart Manufacturing, *ACS Energy Lett.*, 2020, **5**, 3069–3100.

30 J. Huang, Y. Yuan, Y. Shao and Y. Yan, Understanding the physical properties of hybrid perovskites for photovoltaic applications, *Nat. Rev. Mater.*, 2017, **2**, 17042.

31 C. H. Lu, G. V. Biesold, Y. J. Liu, Z. T. Kang and Z. Q. Lin, Doping and ion substitution in colloidal metal halide perovskite nanocrystals, *Chem. Soc. Rev.*, 2020, **49**, 4953–5007.

32 Y. R. He, J. X. Yan, L. Xu, B. M. Zhang, Q. Cheng, Y. Cao, J. Zhang, C. Tao, Y. Q. Wei, K. C. Wen, Z. Y. Kuang, G. M. Chow, Z. X. Shen, Q. M. Peng, W. Huang and J. P. Wang, Perovskite Light-Emitting Diodes with Near Unit Internal Quantum Efficiency at Low Temperatures, *Adv. Mater.*, 2021, **33**, 2006302.

33 B. S. B. Karunathilaka, U. Balijapalli, C. A. M. Senevirathne, S. Yoshida, Y. Esaki, K. Goushi, T. Matsushima, A. S. D. Sandanayaka and C. Adachi, Suppression of external quantum efficiency rolloff in organic light emitting diodes by scavenging triplet excitons, *Nat. Commun.*, 2020, **11**, 4926.

34 J. Pan, L. N. Quan, Y. Zhao, W. Peng, B. Murali, S. P. Sarmah, M. Yuan, L. Sinatra, N. M. Alyami, J. Liu, E. Yassitepe, Z. Yang, O. Voznyy, R. Comin, M. N. Hedhili, O. F. Mohammed, Z. H. Lu, D. H. Kim, E. H. Sargent and O. M. Bakr, Highly Efficient Perovskite-Quantum-Dot Light-Emitting Diodes by Surface Engineering, *Adv. Mater.*, 2016, **28**, 8718–8725.

35 X. Y. Shen, Y. Zhang, S. V. Kershaw, T. S. Li, C. C. Wang, X. Y. Zhang, W. Y. Wang, D. G. Li, Y. H. Wang, M. Lu, L. J. Zhang, C. Sun, D. Zhao, G. S. Qin, X. Bai, W. W. Yu and A. L. Rogach, Zn-Alloyed $CsPbI_3$ Nanocrystals for Highly Efficient Perovskite Light-Emitting Devices, *Nano Lett.*, 2019, **19**, 1552–1559.

36 J. H. Li, J. W. Chen, L. M. Xu, S. N. Liu, S. Lan, X. S. Li and J. Z. Song, A zinc non-halide dopant strategy enables efficient perovskite $CsPbI_3$ quantum dot-based light-emitting diodes, *Mater. Chem. Front.*, 2020, **4**, 1444–1453.

37 S. C. Hou, M. K. Gangishetty, Q. M. Quan and D. N. Congreve, Efficient Blue and White Perovskite Light-Emitting Diodes *via* Manganese Doping, *Joule*, 2018, **2**, 2421–2433.

38 B.-B. Zhang, S. Yuan, J.-P. Ma, Y. Zhou, J. Hou, X. Chen, W. Zheng, H. Shen, X.-C. Wang, B. Sun, O. M. Bakr, L.-S. Liao and H.-T. Sun, General Mild Reaction Creates Highly Luminescent Organic-Ligand-Lacking Halide Perovskite Nanocrystals for Efficient Light-Emitting Diodes, *J. Am. Chem. Soc.*, 2019, **141**, 15423–15432.

39 S. Zou, Y. Liu, J. Li, C. Liu, R. Feng, F. Jiang, Y. Li, J. Song, H. Zeng, M. Hong and X. Chen, Stabilizing Cesium Lead Halide Perovskite Lattice through Mn (II)-Substitution for Air-Stable Light-Emitting Diodes, *J. Am. Chem. Soc.*, 2017, **139**, 11443–11450.

40 X. Zhu, L. Ge, Y. Wang, M. Li, R. Q. Zhang, M. C. Xu, Z. H. Zhao, W. Z. Lv and R. F. Chen, Recent Advances in Enhancing and Enriching the Optical Properties of Cl-Based $CsPbX_3$ Nanocrystals, *Adv. Opt. Mater.*, 2021, **9**, 2100058.

41 Y. Zhou, J. Chen, O. M. Bakr and H. T. Sun, Metal-Doped Lead Halide Perovskites: Synthesis, Properties, and Optoelectronic Applications, *Chem. Mater.*, 2018, **30**, 6589–6613.
42 M. V. Kovalenko, L. Protesescu and M. I. Bodnarchuk, Properties and potential optoelectronic applications of lead halide perovskite nanocrystals, *Science*, 2017, **358**, 745–750.
43 Z. Liu, X. Qin, Q. H. Chen, T. C. Jiang, Q. S. Chen and X. G. Liu, Metal-Halide Perovskite Nanocrystal Superlattice: Self-Assembly and Optical Fingerprints, *Adv. Mater.*, 2023, **35**, e2209279.
44 J. Xu, S. Yu, X. Shang and X. Chen, Temperature Dependence of Bandgap in Lead-Halide Perovskites with Corner-Sharing Octahedra, *Adv. Photon. Res.*, 2023, **4**, 2200193.
45 H. H. Yao, J. Zhao, Z. Z. Li, Z. P. Ci and Z. W. Jin, Research and progress of black metastable phase $CsPbI_3$ solar cells, *Mater. Chem. Front.*, 2021, **5**, 1221–1235.
46 Q. J. Gao, J. H. Qi, K. Chen, M. H. Xia, Y. Hu, A. Y. Mei and H. W. Han, Halide Perovskite Crystallization Processes and Methods in Nanocrystals, Single Crystals, and Thin Films, *Adv. Mater.*, 2022, **34**, 2200720.
47 J. Ren, X. Zhou and Y. Wang, Water triggered interfacial synthesis of highly luminescent $CsPbX_3$:$Mn^{2+}$ quantum dots from nonluminescent quantum dots, *Nano Res.*, 2020, **13**, 3387–3395.
48 Y. Tong, E. Bladt, M. F. Aygüler, A. Manzi, K. Z. Milowska, V. A. Hintermayr, P. Docampo, S. Bals, A. S. Urban, L. Polavarapu and J. Feldmann, Highly Luminescent Cesium Lead Halide Perovskite Nanocrystals with Tunable Composition and Thickness by Ultrasonication, *Angew. Chem., Int. Ed.*, 2016, **55**, 13887–13892.
49 D. J. Kubicki, D. Prochowicz, A. Hofstetter, B. J. Walder and L. Emsley, Cd-113 Solid-State NMR at 21.1 T Reveals the Local Structure and Passivation Mechanism of Cadmium in Hybrid and All-Inorganic Halide Perovskites, *ACS Energy Lett.*, 2020, **5**, 2964–2971.
50 T. Guner, B. Akbali, M. Ozcan, G. Topcu, M. M. Demir and H. Sahin, Monitoring the Doping and Diffusion Characteristics of Mn Dopants in Cesium Lead Halide Perovskites, *J. Phys. Chem. C*, 2018, **122**, 11543–11549.
51 F. Bateni, R. W. Epps, K. Abdel-latif, R. Dargis, S. Han, A. A. Volk, M. Ramezani, T. Cai, O. Chen and M. Abolhasani, Ultrafast cation doping of perovskite quantum dots in flow, *Matter*, 2021, **4**, 2429–2447.
52 J. R. Zhu, X. L. Yang, Y. H. Zhu, Y. W. Wang, J. Cai, J. H. Shen, L. Y. Sun and C. Z. Li, Room-Temperature Synthesis of Mn-Doped Cesium Lead Halide Quantum Dots with High Mn Substitution Ratio, *J. Phys. Chem. Lett.*, 2017, **8**, 4167–4171.
53 C. Otero-Martinez, J. Z. Ye, J. Sung, I. Pastoriza-Santos, J. Perez-Juste, Z. G. Xia, A. Rao, R. L. Z. Hoye and L. Polavarapu, Colloidal Metal-Halide Perovskite Nanoplatelets: Thickness-Controlled Synthesis, Properties, and Application in Light-Emitting Diodes, *Adv. Mater.*, 2022, **34**, 2107105.
54 Z. Y. Zhu, Q. Q. Yang, L. F. Gao, L. Zhang, A. Y. Shi, C. L. Sun, Q. Wang and H. L. Zhang, Solvent-Free Mechanosynthesis of Composition-Tunable Cesium Lead Halide Perovskite Quantum Dots, *J. Phys. Chem. Lett.*, 2017, **8**, 1610–1614.
55 K. Abdel-Latif, R. W. Epps, C. B. Kerr, C. M. Papa, F. N. Castellano and M. Abolhasani, Facile Room-Temperature Anion Exchange Reactions of Inorganic Perovskite Quantum Dots Enabled by a Modular Microfluidic Platform, *Adv. Funct. Mater.*, 2019, **29**, 1900712.
56 D. Parobek, B. J. Roman, Y. Dong, H. Jin, E. Lee, M. Sheldon and D. H. Son, Exciton-to-Dopant Energy Transfer in Mn-Doped Cesium Lead Halide Perovskite Nanocrystals, *Nano Lett.*, 2016, **16**, 7376–7380.
57 W. Liu, Q. Lin, H. Li, K. Wu, I. Robel, J. M. Pietryga and V. I. Klimov, $Mn^{2+}$-Doped Lead Halide Perovskite Nanocrystals with Dual-Color Emission Controlled by Halide Content, *J. Am. Chem. Soc.*, 2016, **138**, 14954–14961.
58 Q. A. Akkerman, D. Meggiolaro, Z. Dang, F. De Angelis and L. Manna, Fluorescent Alloy $CsPb_xMn_{1-x}I_3$ Perovskite Nanocrystals with High Structural and Optical Stability, *ACS Energy Lett.*, 2017, **2**, 2183–2186.
59 P. Arunkumar, H. B. Cho, K. H. Gil, S. Unithrattil, Y. H. Kim and W. Bin Im, Probing Molecule-Like Isolated Octahedra *via*-Phase Stabilization of Zero-Dimensional Cesium Lead Halide Nanocrystals, *Nat. Commun.*, 2018, **9**, 4691.
60 H. Liu, Z. Wu, J. Shao, D. Yao, H. Gao, Y. Liu, W. Yu, H. Zhang and B. Yang, $CsPb_xMn_{1-x}Cl_3$ Perovskite Quantum Dots with High Mn Substitution Ratio, *ACS Nano*, 2017, **11**, 2239–2247.
61 J. Meng, Z. Y. Lan, M. Abdellah, B. Yang, S. Mossin, M. L. Liang, M. Naumova, Q. Shi, S. L. G. Alvarez, Y. Liu, W. H. Lin, I. E. Castelli, S. E. Canton, T. Pullerits and K. B. Zheng, Modulating Charge-Carrier Dynamics in Mn-Doped All-Inorganic Halide Perovskite Quantum Dots through the Doping-Induced Deep Trap States, *J. Phys. Chem. Lett.*, 2020, **11**, 3705–3711.
62 G. G. Huang, C. L. Wang, S. H. Xu, S. F. Zong, J. Lu, Z. Y. Wang, C. G. Lu and Y. P. Cui, Postsynthetic Doping of $MnCl_2$ Molecules into Preformed $CsPbBr_3$ Perovskite Nanocrystals *via* a Halide Exchange-Driven Cation Exchange, *Adv. Mater.*, 2017, **29**, 1700095.
63 S. Das Adhikari, R. K. Behera, S. Bera and N. Pradhan, Presence of Metal Chloride for Minimizing the Halide Deficiency and Maximizing the Doping Efficiency in Mn(II)-Doped $CsPbCl_3$ Nanocrystals, *J. Phys. Chem. Lett.*, 2019, **10**, 1530–1536.
64 Y. C. Li, C. Y. Wang, G. C. Hu, W. Meng, S. Q. Sui and Z. T. Deng, Promoting the doping efficiency and photoluminescence quantum yield of Mn-doped perovskite nanocrystals *via* two-step hot-injection, *Chem. Commun.*, 2022, **58**, 941–944.
65 J. P. Ma, Y. M. Chen, L. M. Zhang, S. Q. Guo, J. D. Liu, H. Li, B. J. Ye, Z. Y. Li, Y. Zhou, B. B. Zhang, O. M. Bakr, J. Y. Zhang and H. T. Sun, Insights into the local structure of dopants, doping efficiency, and luminescence properties of lanthanide-doped $CsPbCl_3$ perovskite nanocrystals, *J. Mater. Chem. C*, 2019, **7**, 3037–3048.

 

66 S. Das Adhikari, S. K. Dutta, A. Dutta, A. K. Guria and N. Pradhan, Chemically Tailoring the Dopant Emission in Manganese-Doped $CsPbCl_3$ Perovskite Nanocrystals, *Angew. Chem., Int. Ed.*, 2017, **56**, 8746–8750.

67 S. Zhou, Y. W. Zhu, J. S. Zhong, F. F. Tian, H. Huang, J. K. Chen and D. Q. Chen, Chlorine-additive-promoted incorporation of $Mn^{2+}$ dopants into CsPbCl3 perovskite nanocrystals, *Nanoscale*, 2019, **11**, 12465–12470.

68 S. Das Adhikari, A. Dutta, S. K. Dutta and N. Pradhan, Layered Perovskites $L\text{-}_2(Pb_{1-X}Mn_X)C1_4$ to Mn-Doped $CsPbCl_3$ Perovskite Platelets, *ACS Energy Lett.*, 2018, **3**, 1247–1253.

69 W. J. Mir, M. Jagadeeswararao, S. Das and A. Nag, Colloidal Mn-Doped Cesium Lead Halide Perovskite Nanoplatelets, *ACS Energy Lett.*, 2017, **2**, 537–543.

70 S. K. Dutta and N. Pradhan, Coupled Halide-Deficient and Halide-Rich Reaction System for Doping in Perovskite Armed Nanostructures, *J. Phys. Chem. Lett.*, 2019, **10**, 6788–6793.

71 N. Pradhan, Alkylammonium Halides for Facet Reconstruction and Shape Modulation in Lead Halide Perovskite Nanocrystals, *Acc. Chem. Res.*, 2021, **54**, 1200–1208.

72 H. M. Li, W. Dong, X. Y. Shen, C. D. Ge, Y. L. Song, Z. S. Wang, A. R. Wang, Z. Q. Yang, M. W. Hao, Y. Zhang, W. T. Zheng, X. Y. Zhang and Q. F. Dong, Enhancing the Efficiency and Stability of $CsPbI_3$ Nanocrystal-Based Light-Emitting Diodes through Ligand Engineering with Octylamine, *J. Phys. Chem. C*, 2022, **126**, 1085–1093.

73 S. Zhang, L. F. Yuan, H. L. Liu, G. F. Zhou, W. G. Ding, Z. P. Qin, X. G. Li and S. R. Wang, Tunable White Light-Emitting Devices Based on Unilaminar High-Efficiency $Zn^{2+}$-Doped Blue $CsPbBr_3$ Quantum Dots, *J. Phys. Chem. Lett.*, 2021, **12**, 8507–8512.

74 Y. Li, Q. S. Liu, X. J. Liu, J. Feng, L. J. He, H. W. Li, C. Y. Li and H. J. Zhang, Simultaneous Enhancement of Photoluminescence and Stability of $CsPbCl_3$ Perovskite Enabled by Titanium Ion Dopant, *J. Phys. Chem. Lett.*, 2021, **12**, 10746–10752.

75 A. De, S. Das, N. Mondal and A. Samanta, Highly Luminescent Violet- and Blue-Emitting Stable Perovskite Nanocrystals, *ACS Mater. Lett.*, 2019, **1**, 116–122.

76 R. K. Behera, A. Dutta, D. Ghosh, S. Bera, S. Bhattacharyya and N. Pradhan, Doping the Smallest Shannon Radii Transition Metal Ion Ni(II) for Stabilizing alpha-$CsPbI_3$ Perovskite Nanocrystals, *J. Phys. Chem. Lett.*, 2019, **10**, 7916–7921.

77 X. Chen, Z. G. Sun, B. Cai, X. M. Li, S. H. Zhang, D. Fu, Y. S. Zou, Z. Y. Fan and H. B. Zeng, Substantial Improvement of Operating Stability by Strengthening Metal-Halogen Bonds in Halide Perovskites, *Adv. Funct. Mater.*, 2022, **32**, 2112129.

78 Z. Yong, S. Guo, J. Ma, J. Zhang, Z. Li, Y. Chen, B. Zhang, Y. Zhou, J. Shu, J. Gu, L. Zheng, O. M. Bakr and H. Sun, Doping-Enhanced Short-Range Order of Perovskite Nanocrystals for Near-Unity Violet Luminescence Quantum Yield, *J. Am. Chem. Soc.*, 2018, **140**, 9942–9951.

79 V. Naresh and N. Lee, Zn(II)-Doped Cesium Lead Halide Perovskite Nanocrystals with High Quantum Yield and Wide Color Tunability for Color-Conversion Light-Emitting Displays, *ACS Appl. Nano Mater.*, 2020, **3**, 7621–7632.

80 L. Zhang, C. Kang, G. Zhang, Z. Pan, Z. Huang, S. Xu, H. Rao, H. Liu, S. Wu, X. Wu, X. Li, Z. Zhu, X. Zhong and A. K. Y. Jen, All-Inorganic $CsPbI_3$ Quantum Dot Solar Cells with Efficiency over 16% by Defect Control, *Adv. Funct. Mater.*, 2021, **31**, 2005930.

81 J. Li, Z. Guo, S. Xiao, Y. Tu, T. He and W. Zhang, Enhanced Performance of Two-Photon Excited Amplified Spontaneous Emission by Cd-Alloyed $CsPbBr_3$ Nanocrystals, *Inorg. Chem.*, 2022, **61**, 4735–4742.

82 R. Wu, Z. Bai, J. Jiang, H. Yao and S. Qin, Research on the photoluminescence properties of $Cu^{2+}$-doped perovskite $CsPbCl_3$ quantum dots, *RSC Adv.*, 2021, **11**, 8430–8436.

83 C. Bi, S. Wang, Q. Li, S. V. Kershaw, J. Tian and A. L. Rogach, Thermally Stable Copper(II)-Doped Cesium Lead Halide Perovskite Quantum Dots with Strong Blue Emission, *J. Phys. Chem. Lett.*, 2019, **10**, 943–952.

84 C. H. Bi, X. J. Sun, X. Huang, S. X. Wang, J. F. Yuan, J. X. Wang, T. Pullerits and J. J. Tian, Stable $CsPb_{1-x}Zn_xI_3$ Colloidal Quantum Dots with Ultralow Density of Trap States for High-Performance Solar Cells, *Chem. Mater.*, 2020, **32**, 6105–6113.

85 M. Imran, V. Caligiuri, M. Wang, L. Goldoni, M. Prato, R. Krahne, L. De Trizio and L. Manna, Benzoyl Halides as Alternative Precursors for the Colloidal Synthesis of Lead-Based Halide Perovskite Nanocrystals, *J. Am. Chem. Soc.*, 2018, **140**, 2656–2664.

86 C. Y. Zhang, Q. Wan, L. K. Ono, Y. Q. Liu, W. L. Zheng, Q. G. Zhang, M. M. Liu, L. Kong, L. Li and Y. B. Qi, Narrow-Band Violet-Light-Emitting Diodes Based on Stable Cesium Lead Chloride Perovskite Nanocrystals, *ACS Energy Lett.*, 2021, **6**, 3545–3554.

87 D. P. Nenon, K. Pressler, J. Kang, B. A. Koscher, J. H. Olshansky, W. T. Osowiecki, M. A. Koc, L.-W. Wang and A. P. Alivisatos, Design Principles for Trap-Free $CsPbX_3$ Nanocrystals: Enumerating and Eliminating Surface Halide Vacancies with Softer Lewis Bases, *J. Am. Chem. Soc.*, 2018, **140**, 17760–17772.

88 N. Pradhan, Tips and Twists in Making High Photoluminescence Quantum Yield Perovskite Nanocrystals, *ACS Energy Lett.*, 2019, **4**, 1634–1638.

89 Y. Zhang, X. Cheng, D. Tu, Z. Gong, R. Li, Y. Yang, W. Zheng, J. Xu, S. Deng and X. Chen, Engineering the Bandgap and Surface Structure of $CsPbCl_3$ Nanocrystals to Achieve Efficient Ultraviolet Luminescence, *Angew. Chem., Int. Ed.*, 2021, **60**, 9693–9698.

90 T. Cai, H. Yang, K. Hills-Kimball, J.-P. Song, H. Zhu, E. Hofman, W. Zheng, B. M. Rubenstein and O. Chen, Synthesis of All-Inorganic Cd-Doped $CsPbCl_3$ Perovskite Nanocrystals with Dual-Wavelength Emission, *J. Phys. Chem. Lett.*, 2018, **9**, 7079–7084.

91 T. Cai, J. Y. Wang, W. H. Li, K. Hills-Kimball, H. J. Yang, Y. Nagaoka, Y. C. Yuan, R. Zia and O. Chen, $Mn^{2+}/Yb^{3+}$

Codoped $CsPbCl_3$ Perovskite Nanocrystals with Triple-Wavelength Emission for Luminescent Solar Concentrators, *Adv. Sci.*, 2020, **7**, 2001317.

92 W. Zhang, J. Wei, Z. Gong, P. Huang, J. Xu, R. Li, S. Yu, X. Cheng, W. Zheng and X. Chen, Unveiling the Excited-State Dynamics of $Mn^{2+}$ in 0D $Cs_4PbCl_6$ Perovskite Nanocrystals, *Adv. Sci.*, 2020, **7**, 2002210.

93 B. J. Beberwyck, Y. Surendranath and A. P. Alivisatos, Cation Exchange: A Versatile Tool for Nanomaterials Synthesis, *J. Phys. Chem. C*, 2013, **117**, 19759–19770.

94 S. Gupta, S. V. Kershaw and A. L. Rogach, 25th Anniversary Article: Ion Exchange in Colloidal Nanocrystals, *Adv. Mater.*, 2013, **25**, 6923–6943.

95 W. van der Stam, E. Bladt, F. T. Rabouw, S. Bals and C. D. Donega, Near-Infrared Emitting $CuInSe_2/CuInS_2$ Dot Core/Rod Shell Heteronanorods by Sequential Cation Exchange, *ACS Nano*, 2015, **9**, 11430–11438.

96 H. B. Li, R. Brescia, R. Krahne, G. Bertoni, M. J. P. Alcocer, C. D'Andrea, F. Scotognella, F. Tassone, M. Zanella, M. De Giorgi and L. Manna, Blue-UV-Emitting ZnSe(Dot)/ZnS(Rod) Core/Shell Nanocrystals Prepared from CdSe/CdS Nanocrystals by Sequential Cation Exchange, *ACS Nano*, 2012, **6**, 1637–1647.

97 L. De Trizio and L. Manna, Forging Colloidal Nanostructures *via* Cation Exchange Reactions, *Chem. Rev.*, 2016, **116**, 10852–10887.

98 G. Nedelcu, L. Protesescu, S. Yakunin, M. I. Bodnarchuk, M. J. Grotevent and M. V. Kovalenko, Fast Anion-Exchange in Highly Luminescent Nanocrystals of Cesium Lead Halide Perovskites ($CsPbX_3$, X = Cl, Br, I), *Nano Lett.*, 2015, **15**, 5635–5640.

99 W. van der Stam, J. J. Geuchies, T. Altantzis, K. H. W. van den Bos, J. D. Meeldijk, S. Van Aert, S. Bals, D. Vanmaekelbergh and C. D. M. Donega, Highly Emissive Divalent-Ion-Doped Colloidal $CsPb_{1-x}M_xBr_3$ Perovskite Nanocrystals through Cation Exchange, *J. Am. Chem. Soc.*, 2017, **139**, 4087–4097.

100 F. Li, Z. Xia, C. Pan, Y. Gong, L. Gu, Q. Liu and J. Z. Zhang, High Br- Content $CsPb(Cl_yBr_{1-y})_3$ Perovskite Nanocrystals with Strong $Mn^{2+}$ Emission through Diverse Cation/Anion Exchange Engineering, *ACS Appl. Mater. Interfaces*, 2018, **10**, 11739–11746.

101 A. Shapiro, M. W. Heindl, F. Horani, M. H. Dahan, J. Tang, Y. Amouyal and E. Lifshitz, Significance of Ni Doping in $CsPbX_3$ Nanocrystals *via* Postsynthesis Cation-Anion Coexchange, *J. Phys. Chem. C*, 2019, **123**, 24979–24987.

102 W. J. Mir, A. Swarnkar and A. Nag, Postsynthesis Mn-doping in $CsPbI_3$ Nanocrystals to Stabilize the Black Perovskite Phase, *Nanoscale*, 2019, **11**, 4278–4286.

103 C. Otero-Martinez, M. Imran, N. J. Schrenker, J. Z. Ye, K. Y. Ji, A. Rao, S. D. Stranks, R. L. Z. Hoye, S. Bals, L. Manna, J. Perez-Juste and L. Polavarapu, Fast A-Site Cation Cross-Exchange at Room Temperature: Single-to Double- and Triple-Cation Halide Perovskite Nanocrystals, *Angew. Chem., Int. Ed.*, 2022, **61**, e202205617.

104 K. M. Hills-Kimball, M. J. Perez, Y. Nagaoka, T. Cai, H. J. Yang, A. H. Davis, W. W. Zheng and O. Chen, Ligand Engineering for $Mn^{2+}$ Doping Control in $CsPbCl_3$ Perovskite Nanocrystals *via* a Quasi-Solid-Solid Cation Exchange Reaction, *Chem. Mater.*, 2020, **32**, 2489–2500.

105 L. Z. Wu, Y. Wang, M. Kurashvili, A. Dey, M. H. Cao, M. Doblinger, Q. Zhang, J. Feldmann, H. Huang and T. Debnath, Interfacial Manganese-Doping in $CsPbBr_3$ Nanoplatelets by Employing a Molecular Shuttle, *Angew. Chem., Int. Ed.*, 2022, **61**, e202115852.

106 Z. Yang, M. Wei, O. Voznyy, P. Todorovic, M. Liu, R. Quintero-Bermudez, P. Chen, J. Z. Fan, A. H. Proppe, L. N. Quan, G. Walters, H. Tan, J.-W. Chang, U. S. Jeng, S. O. Kelley and E. H. Sargent, Anchored Ligands Facilitate Efficient B-Site Doping in Metal Halide Perovskites, *J. Am. Chem. Soc.*, 2019, **141**, 8296–8305.

107 T. Qiao, D. Parobek, Y. Dong, E. Ha and D. H. Son, Photo-induced Mn doping in cesium lead halide perovskite nanocrystals, *Nanoscale*, 2019, **11**, 5247–5253.

108 F. Li, Y. Liu, H. Wang, Q. Zhan, Q. Liu and Z. Xia, Postsynthetic Surface Trap Removal of $CsPbX_3$ (X = CI, Br, or I) Quantum Dots *via* a $ZnX_2$/Hexane Solution toward an Enhanced Luminescence Quantum Yield, *Chem. Mater.*, 2018, **30**, 8546–8554.

109 C. Xie, Y. Zhao, W. Shi and P. Yang, Postsynthetic Surface-Treatment of $CsPbX_3$ (X = Cl, Br, or I) Nanocrystals *via* $CdX_2$ Precursor Solution toward High Photoluminescence Quantum Yield, *Langmuir*, 2021, **37**, 1183–1193.

110 X. Li, Y. Wu, S. Zhang, B. Cai, Y. Gu, J. Song and H. Zeng, $CsPbX_3$ Quantum Dots for Lighting and Displays: Room-Temperature Synthesis, Photoluminescence Superiorities, Underlying Origins and White Light-Emitting Diodes, *Adv. Funct. Mater.*, 2016, **26**, 2435–2445.

111 K. Xu, E. T. Vickers, B. B. Luo, A. C. Allen, E. F. Chen, G. Roseman, Q. H. Wang, D. S. Kliger, G. L. Millhauser, W. J. Yang, X. M. Li and J. Z. Zhang, First Synthesis of Mn-Doped Cesium Lead Bromide Perovskite Magic Sized Clusters at Room Temperature, *J. Phys. Chem. Lett.*, 2020, **11**, 1162–1169.

112 K. Y. Xu, C. C. Lin, X. B. Xie and A. Meijerink, Efficient and Stable Luminescence from $Mn^{2+}$ in Core and Core-Isocrystalline Shell $CsPbCl_3$ Perovskite Nanocrystals, *Chem. Mater.*, 2017, **29**, 4265–4272.

113 Q. Shan, J. Song, Y. Zou, J. Li, L. Xu, J. Xue, Y. Dong, B. Han, J. Chen and H. Zeng, High Performance Metal Halide Perovskite Light-Emitting Diode: From Material Design to Device Optimization, *Small*, 2017, **13**, 1701770.

114 G. C. Pan, X. Bai, W. Xu, X. Chen, Y. Zhai, J. Y. Zhu, H. Shao, N. Ding, L. Xu, B. Dong, Y. L. Mao and H. W. Song, Bright Blue Light Emission of $Ni^{2+}$ Ion-Doped $CsPbCl_xBr_{3-x}$ Perovskite Quantum Dots Enabling Efficient Light-Emitting Devices, *ACS Appl. Mater. Interfaces*, 2020, **12**, 14195–14202.

115 Y. K. Wang, X. Y. Liu, Q. Q. He, G. Y. Chen, D. D. Xu, X. D. Chen, W. B. Zhao, J. C. Bao, X. X. Xu, J. L. Liu and X. Wang, Reversible Transformation between $CsPbBr_3$ Perovskite Nanowires and Nanorods with Polarized Optoelectronic Properties, *Adv. Funct. Mater.*, 2021, **31**, 2011251.

 

116 S. Ye, M. J. Zhao, J. Song and J. L. Qu, Controllable emission bands and morphologies of high-quality $CsPbX_3$ perovsKite nanocrystals prepared in octane, *Nano Res.*, 2018, **11**, 4654–4663.
117 A. Q. Liu, G. Y. Guan, X. M. Chai, N. N. Feng, M. Lu, X. Bai and Y. Zhang, Metal Halide Perovskites toward Electrically Pumped Lasers, *Laser Photon. Rev.*, 2022, **16**, 2200189.
118 C. Otero-Martinez, N. Fiuza-Maneiro and L. Polavarapu, Enhancing the Intrinsic and Extrinsic Stability of Halide Perovskite Nanocrystals for Efficient and Durable Optoelectronics, *ACS Appl. Mater. Interfaces*, 2022, **14**, 34291–34302.
119 A. Matuhina, G. K. Grandhi, M. N. Liu, J. H. Smatt, N. S. M. Viswanath, H. Ali-Loytty, K. Lahtonen and P. Vivo, Octahedral distortion driven by $CsPbI_3$ nanocrystal reaction temperature - the effects on phase stability and beyond, *Nanoscale*, 2021, **13**, 14186–14196.
120 Q. A. Akkerman, G. Raino, M. V. Kovalenko and L. Manna, Genesis, challenges and opportunities for colloidal lead halide perovskite nanocrystals, *Nat. Mater.*, 2018, **17**, 394–405.
121 Y. Wang, G. Chen, D. Ouyang, X. He, C. Li, R. Ma, W.-J. Yin and W. C. H. Choy, High Phase Stability in $CsPbI_3$ Enabled by Pb-I Octahedra Anchors for Efficient Inorganic Perovskite Photovoltaics, *Adv. Mater.*, 2020, **32**, 2000186.
122 J. B. Zhang, L. W. Zhang, P. Cai, X. G. Xue, M. K. Wang, J. Zhang and G. L. Tu, Enhancing stability of red perovskite nanocrystals through copper substitution for efficient light-emitting diodes, *Nano Energy*, 2019, **62**, 434–441.
123 J. Y. Woo, Y. Kim, J. Bae, T. G. Kim, J. W. Kim, D. C. Lee and S. Jeong, Highly Stable Cesium Lead Halide Perovskite Nanocrystals through in Situ Lead Halide Inorganic Passivation, *Chem. Mater.*, 2017, **29**, 7088–7092.
124 H. Yang, W. Yin, W. Dong, L. Gao, C.-H. Tan, W. Li, X. Zhang and J. Zhang, Enhancing the light-emitting performance and stability in $CsPbBr_3$ perovskite quantum dots *via* simultaneous doping and surface passivation, *J. Mater. Chem. C*, 2020, **8**, 14439–14445.
125 X. Chen, K. Xing, Z. Cao, X. Yuan and J. Zhao, Improving Thermal Stability of Photoluminescence in Violet-emitting $CsPbCl_3$ Perovskite Nanocrystals Using Ni Doping, *Chin. J. Lumin.*, 2019, **40**, 1220–1227.
126 M. Xie, J. Guo, X. Zhang, C. Bi, L. Zhang, Z. Chu, W. Zheng, J. You and J. Tian, High-Efficiency Pure-Red Perovskite Quantum-Dot Light-Emitting Diodes, *Nano Lett.*, 2022, **22**, 8266–8273.
127 J. K. Lyu, B. Dong, G. C. Pan, L. H. Sun, X. Bai, S. T. Hu, B. Shen, B. S. Zhou, L. Wang, W. Xu, D. L. Zhou, L. Xu and H. W. Song, $Ni^{2+}$ and $Pr^{3+}$ Co-doped $CsPbCl_3$ perovskite quantum dots with efficient infrared emission at 1300 nm, *Nanoscale*, 2021, **13**, 16598–16607.
128 K. Xing, X. Yuan, Y. Wang, J. Li, Y. J. Wang, Y. Fan, L. Yuan, K. Li, Z. J. Wu, H. B. Li and J. L. Zhao, Improved Doping and Emission Efficiencies of Mn-Doped $CsPbCl_3$ Perovskite Nanocrystals *via* Nickel Chloride, *J. Phys. Chem. Lett.*, 2019, **10**, 4177–4184.
129 P. J. Song, B. Qiao, D. D. Song, J. Y. Cao, Z. H. Shen, Z. Xu, S. L. Zhao, S. Wageh and A. Al-Ghamdi, Modifying the Crystal Field of $CsPbCl_3$:$Mn^{2+}$ Nanocrystals by Co-doping to Enhance Its Red Emission by a Hundredfold, *ACS Appl. Mater. Interfaces*, 2020, **12**, 30711–30719.
130 J. K. Zhang, Y. Z. Zheng, G. T. Liu, Y. Z. Ma, L. Gong, R. Q. Guan, X. Y. Cui, J. J. Yan, J. L. Zhao and J. H. Yang, Pressure-Engineered Optical and Charge Transport Properties of $Mn^{2+}$/$Cu^{2+}$ Codoped $CsPbCl_3$ Perovskite Nanocrystals *via* Structural Progression, *ACS Appl. Mater. Interfaces*, 2020, **12**, 48225–48236.
131 S. Paul, E. Bladt, A. F. Richter, M. Doblinger, Y. Tong, H. Huang, A. Dey, S. Bals, T. Debnath, L. Polavarapu and J. Feldmann, Manganese-Doping-Induced Quantum Confinement within Host Perovskite Nanocrystals through Ruddlesden-Popper Defects, *Angew. Chem., Int. Ed.*, 2020, **59**, 6794–6799.
132 Z. Song, J. Zhao and Q. Liu, Luminescent perovskites: recent advances in theory and experiments, *Inorg. Chem. Front.*, 2019, **6**, 2969–3011.
133 L. Chouhan, S. Ghimire, C. Subrahmanyam, T. Miyasaka and V. Biju, Synthesis, optoelectronic properties and applications of halide perovskites, *Chem. Soc. Rev.*, 2020, **49**, 2869–2885.
134 J. Guo, Y. Fu, M. Lu, X. Zhang, S. V. Kershaw, J. Zhang, S. Luo, Y. Li, W. W. Yu, A. L. Rogach, L. Zhang and X. Bai, Cd-Rich Alloyed $CsPb_{1-x}Cd_xBr_3$ Perovskite Nanorods with Tunable Blue Emission and Fermi Levels Fabricated through Crystal Phase Engineering, *Adv. Sci.*, 2020, **7**, 2000930.
135 M. Imran, J. Ramade, F. Di Stasio, M. De Franco, J. Buha, S. Van Aert, L. Goldoni, S. Lauciello, M. Prato, I. Infante, S. Bals and L. Manna, Alloy $CsCd_xPb_{1-x}Br_3$ Perovskite Nanocrystals: The Role of Surface Passivation in Preserving Composition and Blue Emission, *Chem. Mater.*, 2020, **32**, 10641–10652.
136 C. Zhang, B. Wang, Q. Wan, L. Kong, W. Zheng, Z. Li and L. Li, Critical role of metal ions in surface engineering toward brightly luminescent and stable cesium lead bromide perovskite quantum dots, *Nanoscale*, 2019, **11**, 2602–2607.
137 G. H. Ahmed, Y. Liu, I. Bravic, X. Ng, I. Heckelmann, P. Narayanan, M. S. Fernandez, B. Monserrat, D. N. Congreve and S. Feldmann, Luminescence Enhancement Due to Symmetry Breaking in Doped Halide Perovskite Nanocrystals, *J. Am. Chem. Soc.*, 2022, **144**, 15862–15870.
138 K. R. Pradeep, D. Acharya, P. Jain, K. Gahlot, A. Yadav, A. Camellini, M. Zavelani-Rossi, G. Cerullo, C. Narayana, S. Narasimhan and R. Viswanatha, Harvesting Delayed Fluorescence in Perovskite Nanocrystals Using Spin-Forbidden Mn d States, *ACS Energy Lett.*, 2020, **5**, 353–359.